Inaugural dissertation

for

obtaining the doctoral degree

of the

Combined Faculty of Mathematics, Engineering and Natural Sciences

of the

Ruprecht - Karls - University

Heidelberg

Presented by

M.Sc. Leon Heine

born in: Bremen, Germany

Oral examination: 02.02.2026

TIR-domain-containing protein C of uropathogenic *E. coli* CFT073 as a modulator of innate immune checkpoints

Referees: Prof. Dr. Nina Papavasiliou

Prof. Dr. med. Thomas Miethke

Parts of this thesis are currently in revision to be published:

Heine L., Griffith H., Hu H., Müller I., Kuhn S., Rudolph L., Rait X., Waldhuber A., Chen Y., Miethke T.: “TIR-domain-containing protein C as modulator of innate immune checkpoints.” *Sci Rep*.

Abstract

Urinary tract infections are one of the most common community-acquired infections worldwide, affecting approximately 150 million people each year. Uropathogenic *E. coli* are responsible for the vast majority of UTIs. In order to infect the lower and upper urinary tract, they express a wide variety of virulence factors. One of these virulence factors is TcpC, a Toll/interleukin-1 receptor domain-containing protein produced by various *E. coli* strains of the phylogenetic group B2, including CFT073. Studies have shown that TcpC is able to inhibit TNFα and IL-1β release of mouse macrophages during an infection with *E. coli* CFT073. It is suggested that TcpC is able to inhibit cytokine release of these cells by binding to specific proteins of the TLR4 signaling cascade and the NLRP3 inflammasome.

I now report that TcpC is able to stimulate cytokine release of immune and bladder epithelial cells during infection. Human monocytes and human bladder epithelial cells release higher amounts of proinflammatory cytokines after infection with TcpC-producing CFT073 strains compared to a TcpC knockout. Differentiation of monocytes to macrophages abrogates this TcpC-dependent effect. Infection of T24/83ΔTLR4 cells suggests that exclusively TLR4 is responsible for a proinflammatory reaction. Furthermore, infection of T24/83ΔMyD88 bladder epithelial cells suggests that the TcpC-induced stimulation of proinflammatory cytokines is MyD88-independent. THP-1 cells treated with conditioned medium in which TcpC was overexpressed at different levels showed that TcpC inhibited cytokine release after stimulation with LPS plus ATP at low levels of induction. Deletion of the TIR-domain of TcpC leads to a loss of the inhibitory capabilities, showing that it is crucial for the function of the protein in this context.

Thus, during an infection of monocytes with CFT073, the proinflammatory response is increased compared to the TcpC knockout strain, whereas treatment with culture supernatants containing TcpC inhibits the proinflammatory response of LPS plus ATP stimulated monocytes. In summary, I conclude that the TcpC-induced inhibition versus stimulation of release of proinflammatory cytokines may depend on the direct contact between CFT073 and eukaryotic cells. Since TcpC is able to bind to TLR4 and MyD88, I think it affects myddosome formation after stimulation of cells with LPS, which may be further influenced by the direct contact of the bacterium with the immune cells.

Zusammenfassung

Harnwegsinfektionen sind, mit ungefähr 400 Millionen Betroffenen jährlich, eine der am häufigsten vorkommenden bakteriellen Infektionen. Dabei sind uropathogene *E. coli* die häufigsten Erreger. Um die unteren und oberen Harnwege zu infizieren, produzieren uropathogene *E. coli* ein breites Arsenal an Virulenzfaktoren. Einer dieser Virulenzfaktoren ist TcpC, ein Protein, welches eine TIR Domäne enthält und von mehreren Stämmen der phylogenetischen Gruppe B2 kodiert ist, so zum Beispiel auch von CFT073. Bereits veröffentlichte Studien zeigen, dass TcpC die Freisetzung der proinflammatorischen Zytokine TNFα und IL-1β blockieren kann. Die Blockade entsteht wahrscheinlich durch die Bindung von TcpC an Proteine der TLR4 Signalkaskade und des NLRP3 Inflammasoms.

Ich zeige jetzt, dass TcpC die Freisetzung von proinflammatorischen Zytokine während einer Infektion von Monozyten und Blasenepithelzellen, verglichen mit einem TcpC defizienten Stamm, stimulieren kann. Die Differenzierung von Monozyten zu Makrophagen unterbindet diesen TcpC abhängigen Effekt. Die Infektion von T24/83ΔTLR4 Blasenepithelzellen zeigt, dass TLR4 entscheidend für die proinflammatorische Antwort verantwortlich ist. Außerdem zeigt die Infektion von T24/83ΔMyD88 Zellen, dass die durch TcpC verursachte stimulierte Freisetzung von proinflammatorischen Zytokinen auch MyD88 unabhängig entstehen kann. THP-1 Zellen, die mit Kulturüberständen, in denen TcpC überexprimiert wurde, behandelt wurden, zeigen hingegen, dass TcpC auch in der Lage ist eine LPS plus ATP induzierte Stimulation zu blockieren. Die Deletion der TIR Domäne führt zu einem Verlust der blockierenden Funktion und zeigt, dass sie für diese Funktion essenziell ist.

Hier zeige ich, dass TcpC während einer Infektion die Freisetzung von proinflammatorischen Zytokinen stimuliert, wohingegen TcpC in Kulturüberständen die Freisetzung durch eine LPS plus ATP Stimulation blockiert. Daraus schließe ich, dass die durch TcpC verursachte Stimulation versus Blockade der Freisetzung von proinflammatorischen Zytokinen vom direkten Kontakt zwischen Bakterium und Wirtszelle abhängt. Da TcpC sowohl an TLR4 als auch an MyD88 binden kann, denke ich, dass TcpC die Bildung des Myddosoms beeinflusst und dieser Einfluss sich durch den direkten Kontakt zur Wirtzelle weiter verändern kann.

Table of Contents

Table of Figures

List of Tables

Abbrevations

APS	Ammonium persulfate
ASC	Apoptosis-associated speck-like protein containing a CARD
Atc	anhydrotetracycline
ATP	Adenosine triphosphate
BSA	Bovine serum albumin
$CaCl_2$	Calcium chloride
cGAMP	Cyclic guanosine-adenosine monophosphate
cGAS	cGAMP synthase
DAMP	Damage-associated molecular pattern
DMSO	Dimethylsulfideoxide
DNA	Deoxyribonucleic acid
EDTA	Ethylenediaminetetraacetic acid
FACS	Fluorescence-Activated Cell Sorting
FCS	Fetal calf serum
FRT	Flippase recognition target
GAPDH	Glycerinaldehyd-3-phosphat-Dehydrogenase
GM-CSF	Granulocyte-macrophage colony-stimulating factor
IBC	Intracellular bacterial community
IL	Interleukin

IP	Immunoprecipitation
IRAK1/2/4	interleukin-1 receptor-associated kinases 1/2/4
IRF3	Interferon regulatory factor 3
IκB	Inhibitor of NF-κB
KCl	Potassium chloride
LB	Lysogeny broth
LPS	Lipopolysaccharide
MACS	Magnetic-activated cell sorting
MAVS	Mitochondrial antiviral signaling protein
M-CSF	Macrophage colony-stimulating factor
MDA5	Melanoma differentiation factor 5
MDM	Monocyte-derived macrophage
$MgSO_4$	Magnesium sulphate
MIP-2	Macrophage inflammatory protein 2
MOI	Multiplicity of infection
MyD88	Myeloid differentiation primary response 88
Na_2HPO_4	Disodium phosphate
Na_3VO_4	Sodium orthovanadate
NaCl	Sodium chloride
NAD	Nicotinamide adenine dinucleotide
NaF	Sodium fluoride

NF-κB	Nuclear factor kappa-light-chain-enhancer of activated B cells
NLRP3	NOD-like receptor family pyrin domain-containing 3
NP-40	Nonidet P-40
NTP	Nucleoside triphosphate
PBMC	peripheral blood mononuclear cells
PAMP	Pathogen-associated molecular pattern
PAβN	phenylalanine-arginine-β-naphtylamide
PBS	Phosphate-buffered saline
PCR	Polymerase chain reaction
PMA	Phorbol-12-Myristat-13-Acetat
PMSF	Phenylmethylsulfonylfluoride
PMN	Polymorphonuclear leukocytes
PRR	Pattern recognition receptor
RIG-I	Retinoid acid inducible gene I
RLR	(RIG-I)-like receptor
RNA	Ribonucleic acid
SDS	Sodium dodecyl sulfate
SDS-PAGE	SDS-polyacrylamide gel electrophoresis
SMOC	Supramolecular organizing center
SOC	Super optimal broth
STING	Stimulator of interferon genes

TAB1/2	TAK-binding proteins 1/2
TAE	TRIS acetate EDTA
TAK1	Transforming growth factor β-activated kinase 1
TBS	Tris-buffered saline
TBS-T	TBS + Tween20
TcpC	TIR-domain-containing protein C
ThsB	Thermosome subunit beta
TIR	Toll/Interleukin-1 receptor
TIRAP	TIR domain-containing adaptor protein
TLR	Toll-like receptor
TNFα	Tumor necrosis factor-alpha
TRAF6	TNF receptor-associated factor 6
TRIF	TIR-domain-containing adapter-inducing interferon-β
UPEC	Uropathogenic *E. coli*
UTI	Urinary tract infection

1 Introduction

1.1 Urinary tract infections (UTIs)

Urinary tract infections are among the most common infections worldwide. In 2019, an estimated 404 million cases and 237,000 deaths occurred (Yang, et al., 2022), leading to a societal cost of approximately 3.5 billion US dollars (He, et al., 2025). Compared to 1990, both the number of cases and deaths increased by 66% and 190%, respectively. UTIs are common both as community-acquired and healthcare-associated infections. A 2014 study by the Centers for Disease Control and Prevention (CDC) reported that, in the US, 12.9% of all healthcare-associated infections were UTIs (Magill, et al., 2014), while the European Centre for Disease Prevention and Control (ECDC) reported in 2023 that 19.2% of healthcare-associated infections in Europe were UTIs (ECDC, Stockholm). UTIs mainly affect women. Between 50% and 60% of adult women will experience at least one UTI (Medina & Castillo-Pino, 2019), whereas only 20% of men will have at least one UTI during their lifetime (Farrell, et al., 2021). In young sexually active women, the risk of UTI is high, it then decreases in middle-aged women and rises from there with advancing age. In men, the risk of a UTI is considerably lower, and it increases with age (Rowe & Juthani-Mehta, 2013).

The urinary tract consists of the urethra, bladder, ureters, and kidneys. In healthy individuals, most of the urinary tract remains sterile. It is generally protected from microbial colonization by regular urine flow that clears the urethra, along with a mucus layer on the urinary tract, epithelial cells that line every part of the urinary tract, and resident immune cells (Abraham & Miao, 2015). Depending on the location of the bacteria, UTIs can generally be classified as cystitis, an infection of the bladder, pyelonephritis, an infection of the kidneys, or bacteriuria, bacteria in the urine. UTIs can be caused by various gram-negative and gram-positive bacteria, with the most common uropathogen being uropathogenic *E. coli* (UPECs).

1.2 Uropathogenic *E. coli*

UPECs are the cause of approximately 80% of community-acquired UTIs, and many of them naturally populate the gut (Santiago-Borges, et al., 2025, Mediati, et al., 2024). To colonize the urinary tract, they possess specific virulence factors encoded on

pathogenicity islands that differentiate them from commensal *E. coli*. The virulence factors encoded in UPECs can be categorized into surface and secreted virulence factors. Surface virulence factors mainly consist of various adhesins, such as type 1 fimbriae, P fimbriae, and flagella (Shah, et al., 2019). Type 1 fimbriae are associated with improved invasion and biofilm formation. P fimbriae are responsible for the adhesion to the mucosa and tissues inside the urinary tract. They have been shown to be important in the early colonization of the kidney tubular epithelium. Furthermore, P fimbriae contribute to TLR4 activation by binding to glycosphingolipids and the subsequent release of ceramide, a TLR4 agonist (Fischer, et al., 2007). Flagella enable *E. coli* to be motile and help the bacteria to ascend the urinary tract. It has been shown that flagella are needed for the uropathogenic *E. coli* NU149 to ascend to the kidney (Schwan, 2008). LPS is a fundamental component of the outer membrane of Gram-negative bacteria. It consists of three functional parts: lipid A, the core oligosaccharide, and the O-antigen. Lipid A is a hydrophobic structure that anchors the LPS in the outer membrane of the bacteria. It is also the part that is recognized by the TLR4 receptor. The core oligosaccharide links the lipid A with the O-antigen. The O-antigen, together with the oligosaccharide, provides a hydrophilic barrier that protects the bacteria from hydrophobic compounds and is an antigen recognized by the immune system (Bertani & Ruiz, 2018, Domínguez-Medina, et al., 2020).

An important secreted virulence factor is α-hemolysin (HlyA). It has been shown that HlyA can lyse erythrocytes and nucleated host cells at high concentrations. Furthermore, it is able to induce apoptosis in macrophages by activating the NLRP3 inflammasome (Murthy, et al., 2018; Verma, et al., 2020).

During a UTI, these bacteria ascend through the urinary tract and, upon reaching the bladder, can colonize it and cause cystitis (Bien, et al., 2012; Kaper, et al., 2004). Symptoms of a cystitis are often painful and frequent urination, and feeling the need to urinate despite having an empty bladder. From the bladder, bacteria can further ascend the urinary tract to the kidneys, causing pyelonephritis. Symptoms of a pyelonephritis include fever, lower back pain, and nausea or vomiting (CDC, 2025).

1.3 The immune system

The role of the immune system is to protect our bodies from infectious microbes and foreign substances. In addition to protecting us from external threats, it also protects us from our own cells by clearing damaged or dysfunctional cells. An immune response can be triggered by various reasons, such as pathogens, foreign objects entering our body, or mutated malignant cells. To accomplish this, it developed precise and complex processes and a sequence of events to maintain homeostasis. Defects in this system can lead to the immune system attacking our own body called autoimmunity.

The immune system can be categorized into the older, more primitive, and fast-responding innate immune system and the younger, more adaptable, and slower-responding adaptive immune system. The innate immune system is responsible for the response to pathogens in the first hours of infection before the adaptive immune system is able to develop and respond. It reacts to a set of highly conserved foreign patterns with a tool set that is present even before the response starts (Janeway Jr & Medzhitov, 2002). Therefore, the response to these foreign patterns is always the same. Parts of the innate immune system include barriers like epithelia and mucous membranes, phagocytic cells such as neutrophils and macrophages, natural killer cells (NK cells), and proteins like the complement system. The main strategies are the recruitment of phagocytes and other leukocytes, and blocking viral replication or killing of cells that are infected by viruses or bacteria. The adaptive immune response is conveyed by B lymphocytes and T lymphocytes. These cells recognize antigens and are characterized by their specificity and ability to develop antibodies and receptors against an extremely high number of antigens. Upon antigen recognition, B cells undergo clonal selection to create highly specific antibodies that bind the foreign antigens (Rajewsky, 1996). This information can then be preserved in memory B cells so that when the immune system reencounters this specific antigen, the clonal selection does not need to start over. That makes the response to subsequent exposure to the same antigens faster. T cells express the highly specific T cell receptor (TCR) with which they recognize pathogens, immune cells, or other malignant cells. Upon activation, they first undergo clonal expansion, which is why their activity is delayed compared to innate immune cells. After that, they contribute to inflammation by secreting proinflammatory cytokines or recognizing and killing pathogens (Shah, et al., 2021; Sun, et al., 2023). Additionally, T cells provide B cell help functions such as

inducing proliferation and plasma cell differentiation, or improving B cell survival (Crotty, 2015).

Another important feature of the immune system is that, in healthy individuals, it does not develop a response against its own body, and TLRs are not activated by the body's own molecular patterns, and B and T cells recognize the body’s own antigens as harmless (Abbas & Andrew H. Lichtman, 2022).

1.3.1 TLRs

Toll receptors were initially discovered in Drosophila. The activation of Drosophila Toll receptors leads to the translocation of a transcription factor into the nucleus and shows similarities to the mammalian IL-1 signaling pathway. Both the Drosophila Toll receptor and the mammalian IL-1 receptor possess highly conserved motifs called Toll/Interleukin-1 receptor (TIR) domains (Imler & Hoffmann, 2002). One year after the discovery of the Drosophila Toll receptor, homologues to these receptors were discovered in mammals, which are called Toll-like receptors (TLRs) (Takeda, et al., 2003).

TLRs are one of the major groups of receptors in innate immunity, recognizing harmful microbes (Table 1). Humans have 10 different TLRs (Table 1) that are either located on the plasma membrane or endosomes, and they typically consist of three domains: An N-terminal ectodomain that is organized in Leucin-rich repeats (LRRs), a central transmembrane domain, and a C-terminal endodomain consisting of the TIR domain. The LRRs are highly specific for each TLR and are responsible for recognizing the ligands (Matsushima, et al., 2007). The transmembrane domain anchors the receptor in the plasma membrane or the endosomal membrane. The TIR domain is responsible for signal transduction upon activation by binding adaptor proteins, facilitating downstream signaling. Upon activation, TLRs usually form homo- or heterodimers (Sameer & Nissar, 2021; Akira, et al., 2001).

Table 1 List of TLRs

TLRs	Localization	Ligand
TLR1	Plasma membrane	Bacterial lipopeptides
TLR2	Plasma membrane	Bacterial peptidoglycan
TLR3	Endosome	Viral dsRNA
TLR4	Plasma membrane	LPS
TLR5	Plasma membrane	Bacterial flagellin
TLR6	Plasma membrane	Bacterial lipopeptides
TLR7	Endosome	Viral ssRNA
TLR8	Endosome	Viral ssRNA
TLR9	Endosome	Viral, bacterial, and fungal CpG DNA
TLR10	Endosome	Unknown

1.3.2 Cytosolic PRRs

In addition to TLRs as surface or endosomal PRRs, the innate immune system utilizes a variety of cytosolic PRRs that sense PAMPs and DAMPs that have entered the cells. The cytosolic receptors are divided into three major groups: the NOD-like receptors (NLRs), the RIG-like receptors (RLRs), and the DNA sensors of the cGAS-STING pathway (Li, et al., 2021).

NLRs generally consist of a C-terminal LRR, which is responsible for ligand recognition, a central NACHT domain that is required for oligomerization of the NLRs, and an N-terminal effector domain, which activates downstream proteins. They can be further divided into non-inflammasome-forming NLRs and inflammasome-forming NLRPs. The non-inflammasome-forming NLRs typically activate NF-κB; members of this group include NOD1/2 (Caruso, et al., 2014). The inflammasome-forming NLRs interact with the adaptor protein ASC to form so-called supramolecular organizing centers (SMOCs) and activation of the inflammatory caspases-1 and -5. The caspases then facilitate maturation of IL-1β and pyroptosis; members include NLRP3 (Kelley, et al., 2019) and NLRC4 (Matico, et al., 2024).

RLRs are sensors for intracellular virus RNA. They contain a C-terminal domain recognizing dsRNA or RNA-DNA heteroduplexes, an RNA-helicase domain, and two N-terminal caspase recruitment domains, which can activate downstream proteins.

Two members of the RLR family are RIG-I and MDA5. Upon activation, they are recruited to the mitochondrial membrane by MAVS. MAVS then induces the production of type I interferons by activating IRF3, IRF7, and NF-κB (Wicherska-Pawłowska, et al., 2021).

The DNA sensors of the cGAS-STING pathway are activated when cGAS binds to dsDNA. It produces cGAMP, which activates STING and leads to the production of type I interferons through the activation of IRF3 (Zhou, et al., 2023).

1.3.3 TLR4 signaling cascade

MyD88-dependent pathway

TLR4 is activated by LPS binding to a complex that it forms with MD2. To be able to bind the TLR4-MD2 complex, LPS is bound by LPS-binding protein (LBP), which CD14 then captures. CD14 delivers the captured LPS to the TLR4-MD2 complex, leading to the formation of TLR4 homodimers and the subsequent activation of the receptor. That is followed by the recruitment of the TIR domain-containing adaptor proteins Myeloid Differentiation Factor 88 (MyD88) and TIRAP, which then bind IRAK1/2 and IRAK4, leading to their phosphorylation. MyD88, IRAK2, and IRAK4 form a SMOC, the myddosome, consisting of six MyD88, four IRAK2, and four IRAK4 (Gay, et al., 2011). The phosphorylated IRAKs then recruit and bind TRAF6, leading to its polyubiquitination, and TRAF6 then recognizes TAB1, TAB2, and the IKK complex. This activates TAK1, which phosphorylates the IκB complex, causing its degradation and the release of active NF-κB. NF-κB then translocates into the nucleus, where it triggers the production of proinflammatory cytokines like TNFα, IL-6, and IL-8. In addition to proinflammatory cytokines, it also promotes the expression of NLRP3 and immature pro-IL-1β (Kawasaki & Kawai, 2014, Fig. 1).

MyD88-indepentend pathway

While all other TLRs signal through MyD88 as their adaptor protein, TLR3 is the only receptor that solely signals through TRIF. However, TRIF is not restricted to TLR3 as an adaptor protein. It was shown that TLR4 utilized both MyD88 and TRIF to activate both NF-κB and type I interferons (Sato, et al., 2003). Upon activation, TLR4 can be

internalized into endosomes, where the TRIF-dependent pathway of TLR4 can be activated. It was shown that liposomal LPS taken up by cells activated the TRIF-dependent pathway but not the MyD88-dependent pathway (Schultz, et al., 2025; Watanabe, et al., 2013). TRIF is recruited to the endosomal TLR4, then interacts with TRAF3, leading to the phosphorylation of IKKB, TBK1, and IKKε, which activate IRF3 and 7, resulting in type I interferon production (Luo, et al., 2025; Fig. 1) and NF-κB at a late-stage NF-κB activation (Kawai, et al., 2001).

1.3.4 NLRP3 inflammasome

The NLRP3 inflammasome is a SMOC, and upon activation, a single large inflammasome is formed per cell. It is primed by TLR4, through its activation of NF-κB and subsequent induction of NLRP3 and pro-IL-1β expression. NLRP3 is able to sense a variety of DAMPs and PAMPs, including extracellular ATP, K^+-efflux, or bacterial DNA-RNA complexes. Upon activation, NLRP3 oligomerizes with other NLRP3 proteins and binds the adaptor protein ASC. This results in ASC binding more cytosolic ASC, causing filamentation and the formation of a single large inflammasome. ASC then recruits inactive caspase-1, which is activated through proteolysis due to clustering in the inflammasome. Active caspase-1 cleaves inactive pro-IL-1β into active IL-1β. IL-1β does not possess a signal peptide through which the protein can be secreted. It is thought that IL-1β is mainly released during pyroptosis. Pyroptosis is a form of programmed cell death that is also facilitated by the NLRP3 inflammasome. Capsase-1 also cleaves and thereby activates the pore-forming protein gasdermin D. IL-1β can be released through the pores formed by gasdermin D, however, that also leads to cell death due to water influx (Kelley, et al., 2019; Fig. 1).

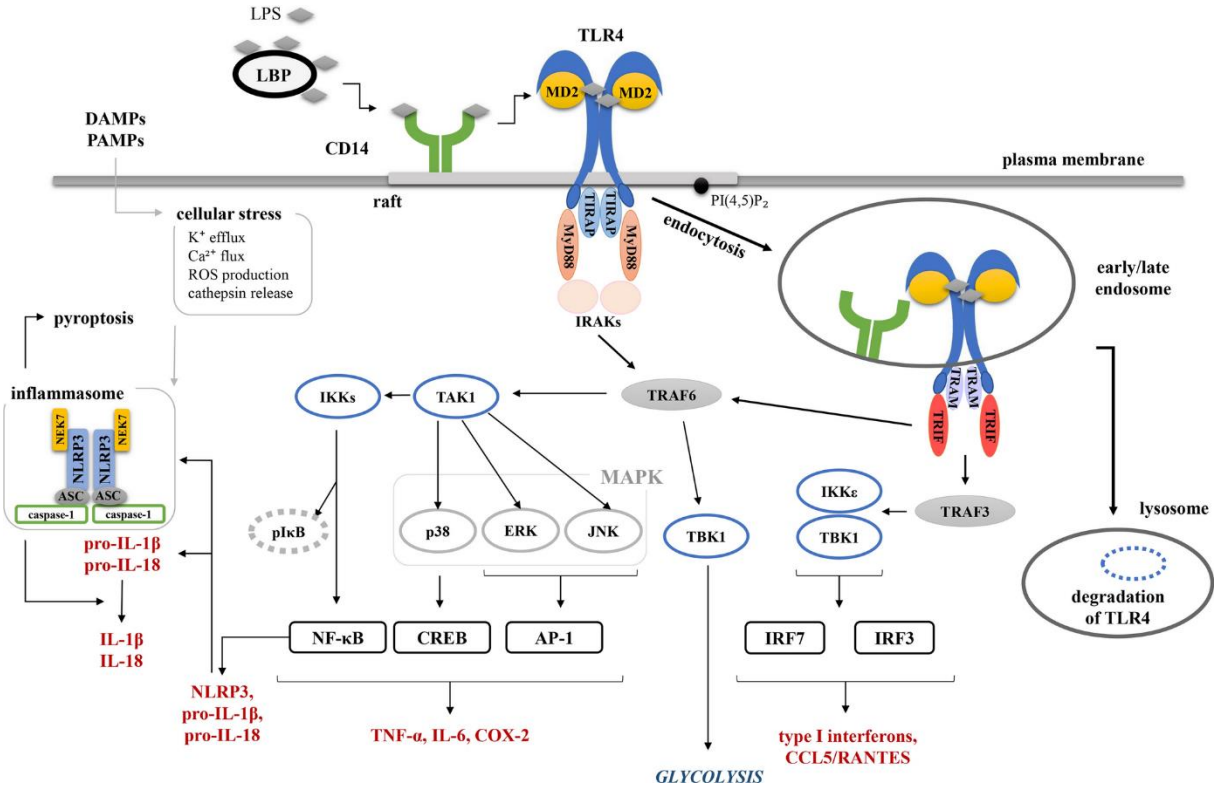

Figure 1 TLR4 and NLRP3 inflammasome signal transduction

Schematic view of the TLR4 receptor and NLRP3 inflammasome pathway. TLR4 is activated on the cell surface, triggering the canonical MyD88-dependent pathway, leading to NF-κB activation and the production of proinflammatory cytokines, as well as NLRP3 and pro-IL-1β. TLR4 can also be internalized, triggering the non-canonical TRIF-dependent pathway that leads to activation of NF-κB and type I interferons. A second signal, such as potassium efflux, activates the NLRP3 inflammasome, leading to the maturation of IL-1β and gasdermin D. Active gasdermin D triggers programmed cell death pyroptosis, which leads to the release of IL-1β. Adapted from Ciesielska, et al., 2021.

1.4 Innate Immunity in UTIs

After UPEC invasion of the urinary tract and the bladder, the first cells to respond are bladder epithelial cells and resident macrophages. These cells generally recognize conserved pathogen-associated molecular patterns (PAMPs) or damage-associated molecular patterns (DAMPs) via pattern recognition receptors (PRRs). Two important families of PRRs in UTI are the Toll-like receptor (TLR) (El-Zayat, et al., 2019) and NOD-like receptor (NLR) families. Two important receptors of these families are the TLR4 receptor, which recognizes LPS, and NLRP3 and its inflammasome, primed by TLR4 activation and assembled by sensing intracellular DNA or cell damage (Zhong, et al., 2013).

Mutations in the promoter of TLR4 are associated with an increased risk of recurrent UTIs in children, and mice deficient in LPS signaling are colonized by up to 1,000-fold

more bacteria in the kidney. TLR5-deficient mice also show higher bacterial numbers in the bladder and kidney 5 days after infection, compared to wild-type mice (Mariano & Ingersoll, 2020). This shows how crucial it is that the UPECs are recognized by TLRs during UTIs. Especially, macrophages play an important role in the immune response as they are nearly 40% of all $CD45^+$ cells in the bladder of mice (Mariano & Ingersoll, 2018). In the first hours of infection, many resident macrophages die due to apoptosis. The consequence is higher monocyte infiltration into the bladder, and pyroptotic macrophages can also entrap bacteria. Although resident macrophages can proliferate and thereby remain in the bladder, resident macrophages that die during infection are often replaced by recruited monocyte-derived macrophages. These monocyte-derived macrophages can then develop into resident macrophages (Mariano, et al., 2020).

By releasing IL-8 after TLR4 activation, epithelial cells and resident macrophages attract neutrophils to the infection site. Neutrophils are the first immune cells to migrate from the blood to the infection site, where they begin neutralizing bacteria using multiple strategies simultaneously. The main processes are phagocytosis, degranulation, and the release of antibacterial compounds, and the release of neutrophil extracellular traps (NETs), where they release their DNA in order to capture bacteria (Kuhn, et al., 2023). Another important immune cell is the monocyte, which arrives at the site of infection shortly after neutrophils. Proinflammatory monocytes migrate to the infection site and initially release IL-6 from bladder epithelial cells, thereby stimulating monocyte proliferation during infection. After migration from the bloodstream to the infection site, monocytes have multiple roles. They produce chemokines and cytokines in response to bacterial PAMPS, mainly LPS. Furthermore, they differentiate into macrophages, which play a key role in phagocytosing bacteria. The presence of macrophages is crucial for regulating the influx of neutrophils. Excessive or prolonged NETosis can lead to tissue damage and chronic inflammation (Naskar & Choi, 2024). During inflammation, many cytokines and chemokines are released, initiating cell migration to the infection site, activating or differentiating immune cells, and later restoring homeostasis.

1.5 TIR-domain-containing proteins in bacteria

TIR domains are structures located in the endodomain of TLRs and IL-1Rs. Upon activation, they form homodimers, causing a conformational change that mediates the

binding of adaptor proteins through TIR-TIR interactions. Mammalian TIR domains are defined through three conserved motifs, the so-called box 1, 2, and 3. Later, Ve, et al., 2017, found that boxes 2 and 3 are actually poorly conserved and question whether this classification should be continued.

Besides, in mammalian proteins, TIR domains also occur in plant and bacterial proteins. In plants, TIR-domain-containing proteins are involved in the host defense against pathogens. Nucleotide-binding LRR proteins contain a N-terminal TIR domain and are responsible for recognizing intracellular PAMPs and initiating an immune response that includes localized cell death (Bernoux, et al., 2011)

It has also been shown that TIR domain proteins are part of the bacterial defense against phages called Theoris, where the TIR domain protein ThsB recognizes phage infection and activates a NADase, depleting the bacteria of NAD^+ and interrupting phage replication (Ofir, et al., 2021). It was also shown that both mammalian and bacterial TIR domains can act as NAD^+ hydrolyses themselves (Doron, et al., 2018; Essuman, et al., 2018).

Furthermore, it was shown that a set of bacterial TIR-domain-containing proteins, including TIR-like protein A (TlpA) of Salmonella enterica, the Yersinia pestis TIR-domain protein TcpB of *Brucella spp.*, and TcpC of several *E. coli* species, are able to interact with part of the innate immune system. All four proteins were shown to be able to interact with mammalian TIR domains of specific TLRs and adaptor proteins and thereby modify the immune response of eukaryotic cells (Snyder, et al., 2014; Li, et al., 2016; Spear, et al., 2012; Rana, et al., 2011; Newman, et al., 2006).

1.6 Role of TcpC in UTIs

During my project, the primary focus lies on the function of TIR-domain-containing protein C (TcpC) of uropathogenic *E. coli* CFT073 during the infection of immune cells and epithelial cells. TcpC is a virulence factor encoded by several *E. coli* strains of the phylogenetic group B2, and its gene is located on the serU pathogenicity island (Vejborg, et al., 2011). TcpC has two main features, a C-terminal transmembrane domain and an N-terminal TIR domain. It has been shown that TcpC can bind TLR4 and its adaptor protein MyD88, as well as the NLRP3 protein and caspase-1 via its TIR domain. A study that looked at bacterial isolates from patients with cystitis and

pyelonephritis found that 22% of isolates from patients with cystitis harbored the TcpC gene, which increased to 44% of isolates in patients with pyelonephritis (Schubert, et al., 2010). This suggests that the ability to express TcpC is beneficial for uropathogenic *E. coli* to ascend the urinary tract and may be associated with greater pathogenicity. This assumption is supported by several studies that examined the role of TcpC during a UTI. The studies showed that 7 days after inducing pyelonephritis in C57BL/6 mice, approximately 75% of mice developed kidney abscesses when infected with TcpC-expressing CFT073. In contrast, no kidney abscesses were observed after infection with a TcpC knockout mutant (Yadav, et al., 2010, Fang, et al., 2021). It is suggested that the more severe disease outcome stems from the ability of TcpC to subvert the innate immune response of mouse macrophages and neutrophils. Infections of mouse macrophages showed that TcpC can inhibit the release of the proinflammatory cytokines IL-1β and TNFα (Cirl, et al., 2008, Waldhuber, et al., 2016). Fang, et al., 2021 suggest that TcpC acts as an E3 ubiquitin ligase that promotes the degradation of MyD88, therefore interrupting the TLR4 signaling cascade. Furthermore, Ou et al. suggest that TcpC can inhibit neutrophil NET formation by promoting the degradation of PAD4 (Ou, et al., 2021)**.** An analysis of the composition of the macrophage population in the kidneys of infected mice also revealed that, in the presence of TcpC, macrophage differentiation into a proinflammatory phenotype was inhibited, whereas differentiation into an anti-inflammatory phenotype was favored (Fang, et al., 2022). These findings indicate that TcpC supports the colonization of the urinary tract of CFT073 by subverting the proinflammatory immune response and thereby impeding bacterial clearance.

In contrast, unpublished data from our lab show that during an infection of bone marrow-derived dendritic cells (BMDCs), TcpC can both inhibit and stimulate IL-1β release compared to a TcpC knockout mutant, depending on the bacterial load. Infection of the human monocyte cell line THP-1 also showed that TcpC stimulates IL-1β release compared with the TcpC knockout mutant, and, interestingly, after differentiation of the THP-1 cells into macrophages, TcpC no longer has an effect during infection.

1.7 Aim of the project

The bacterial virulence factor TcpC is able to modulate the innate immune response. Previous studies showed that TcpC inhibited innate immune responses, which was reflected in a reduction of proinflammatory cytokine release. However, new data suggest that TcpC is also able to stimulate the release of the proinflammatory cytokine IL-1β in human monocytes. The aim of this project is to have a deeper look into the role TcpC plays during infection. Infections of human monocytes and macrophages and bladder epithelial cell lines with TcpC-producing CFT073, the TcpC-deficient CFT073*ΔtcpC,* and the recomplemented CFT073*ΔtcpC*+pTcpC should give new insights into whether TcpC can do more than suppress the innate immune response. The finding in the cell lines will then be validated in primary cells obtained from PBMC of healthy donors. I will also investigate the effect of secreted TcpC on stimulated monocytes by expressing TcpC in culture supernatants, which I will then treat the cells with. With that, I can treat LPS plus ATP stimulated cells with higher amounts of TcpC in a dose-dependent manner without the cytotoxic effect of the bacteria. This thesis will broaden the understanding of the CFT073 virulence factor TcpC, as I describe two contrasting functions of TcpC, its ability to stimulate and impair the release of proinflammatory cytokines in human monocytes and bladder cells depending on the biological circumstances.

2 Material and Methods

2.1 Material

2.1.1 Devices

Agar plate incubator	Binder
Agarose gel electrophoresis system	Peqlab
Autoclave	WTW MultiLab 540
Autoclave	Biomedis
Centrifuges	Hettich Rotixa/P, Hettich Rotina 35R, Hettich Mikro 22R, Eppendorf 5415D
Chemi Doc	Intas ChemoCam ECL-Imager
Clean bench	Heraeus Kendro HS12
Electroporator	Eppendorf Multiporator 4308
FACS	Beckman Coulter Cytoflex S
Freezer (-20°C)	Liebherr
Freezer (-80°C)	Colora, Thermo Fisher
Fridges:	BioBasic, Kirsch, Liebherr
Gel Imager	Intas iX Imager
Heating block	Kisker
Ice machine	Manitowoc
Incubator	Binder, Heraeus
MACS separator	Miltenyi
Microscope	Olympus CK2
Microwave	Sharp R-330A

Milli-Q water filter	Merck
Multi-channel pipette	Brandt
PCR cycler	Biometra T Personal
pH-meter	Biomedis
photometer	Implen OD600
Pipetboy	Integra
Pipettes	Brand
Plate reader	Tecan Spark 10M
PowerPack	Bio-Rad
Scales	Sartorius Extend ED2202S and ED124S
SDS system	Bio-Rad
Semi-dry blotter	Bio-Rad Trans-Blot Turbo Transfer System
Shaker	Biometra WT17
Shaking incubator	GFL
Stepper pipette	Eppendorf
Vortexer	Heidolph Reax2000
Water bath	GFL 1002 and 1004

2.1.2 Consumables

Amicon Ultra Centrifugal Filter (10 kDa mwco)	Merck
Cell culture flasks (T25 and T75)	Sarstedt
Cell culture plates (6-, 24-, and 96-well)	Greiner

Cuvettes	Sarstedt
Electroporation cuvettes	Peqlab
Filter paper	Cytiva
Glassware	Schott
MS columns	Miltenyi
Syringe Needles	BD
Neubauer hemocytometer	Brand
Nitrocellulose membrane (0.22 µm)	Cytiva
PCR tubes	Eppendorf
Protein A agarose beads	Roche
Pipette tips	Brand
Protein A agarose beads	Merck
Reaction tubes 1.5 and 2 ml	Eppendorf, Starlab
Reaction tubes 14 ml	Greiner
Serological pipettes (5 – 25 ml)	Greiner
Sterile filter (0.2 µm)	Sarstedt
Syringes	BD
Falcon Tubes (15 and 50 ml)	Thermo Fisher

2.1.3 Chemicals

2-mercaptoethanol	Sigma-Aldrich
Acetic acid	Carl Roth
Acrylamid 30%	Sigma-Aldrich

Agarose	Invitrogen
Ampicillin	AppliChem
Anhydrotetracycline	Toku-E
APS	Promega
ATP	Carl Roth
Bromophenol blue	Carl Roth
BSA	Carl Roth
$CaCl_2$	Merck
DMSO	Carl Roth
dNTPs	NEB
EDTA	Gibco
Ethanol 99.8%	Carl Roth
Glycerol	Carl Roth
Glycine	Sigma Aldrich
Western Bright Quantum	Advansta
Isopropanol	Carl Roth
Kanamycin	AppliChem
KCl	Sigma-Aldrich
L-arabinose	Sigma-Aldrich
LPS K125	Sigma-Aldrich
Lysozym from eggwhite	Sigma-Aldrich
$MgSO_4$	Merck

Na_2HPO_4	Carl Roth
Na_3VO_4	Sigma-Aldrich
NaCl	Sigma-Aldrich
NaF	AppliChem
NH_4Cl	Merck
Non-fat dry milk powder	AppliChem
Nicotinic acid	Carl Roth
NP-40	Sigma-Aldrich
PMSF	Roche
Protease inhibitor tablets	Sigma-Aldrich
Saponin	Sigma-Aldrich
SDS	Carl Roth
Sodium Deoxycholate	Carl Roth
TEMED	AppliChem
Thiamine	Carl Roth
Tris base	AppliChem
Triton X-100	AppliChem
Trypan blue	Gibco
Tryptone	BD
Tween-20	AppliChem
Yeast extract	BD

2.1.4 Buffers/Solutions/Media

2x Bacterial lysis buffer	100 mM Tris (pH 8.0) 2% SDS 0.2% Triton X-100 20% glycerol
4x Laemmli buffer	250 mM Tris base 280 mM SDS 40% glycerol 20% 2-mercaptoethanol 0.005% bromophenol blue
5x M9 salts (no potassium)	33.9 g/l Na_2HPO_4 2.5 g/l NaCl 5 g/l NH_4Cl
Culture medium	RPMI or McCoy + 10% FCS
Dulbecco's PBS	Sigma-Aldrich
FCS	Gibco
Infection medium	RMPI or McCoy + 3% FCS
IP buffer	50 mM Tris base (pH 7.4) 150 mM NaCl 0.1% NP-40 0.1 mM PMSF 1 mM Na_3VO_4 5 mM NaF 1x protease inhibitor cocktail
LB agar (Lennox)	Carl Roth, 35 g/l
LB medium (Lennox)	Carl Roth, 20 g/l
M9 minimal medium (no potassium)	1x M9 salts 1 mM $MgSO_4$ 0.1 mM $CaCl_2$ 0.4% glucose 0.0025% nicotinic acid 10 g/ml thiamine

MACS buffer	0.5% BSA 2 mM EDTA in PBS
McCoy’s 5 A modified	Gibco or Sigma-Aldrich
RIPA buffer	10 mM Tris (pH 7.4) 1% Triton X-100 1% Sodium Deoxycholate 0.1% SDS, 150 nM NaCl 1 mM PMSF 1 mM Na_3VO_4 5 mM NaF 1x protease inhibitor cocktail
RPMI1640	Gibco
SDS running buffer	25 mM Tris base 192 mM Glycine 0.1% SDS
SOC medium	20 g/l tryptone 5 g/l yeast extract 0.5 g/l NaCl 0.186 g/l KCl
TAE buffer	40 mM Tris (pH 7.4) 20 mM acetic acid 1 mM EDTA
TBS-T	20 mM Tris base 150 mM NaCl 0.1% Tween-20
Transfer buffer	25 mM Tris base 192 mM Glycine 20% Ethanol
Trypsin-EDTA	Carl Roth

2.1.5 Kits

ELISA-Duo Kits	R&D Systems

NucleoSpin Gel and PCR Clean-up	Macherey.Nagel
NucleoSpin Plasmid	Macherey-Nagel
Phusion High-Fidelity DNA-Polymerase	Thermo Fisher
Pierce Coomassie (Bradford) Kit	Thermo Fisher
Rapid DNA Ligation Kit	Thermo Fisher

2.1.6 Enzymes

BsaI restriction enzyme	NEB

2.1.7 Antibodies

CD11b FACS	Miltenyi
CD14 microbeads	Miltenyi
CD45 FACS	Miltenyi
FLAG antibody, mouse	Sigma-Aldrich
GAPDH antibody, mouse	Cell Signaling Technology
IRAK2 antibody, rabbit	Cell Signaling Technology
IRAK4 antibody, rabbit	Cell Signaling Technology
MyD88 antibody, mouse	Cell Signaling Technology
TcpC peptide antibody	Davids Biotechnologie, rabbit serum raised against 35 amino acid fraction of TcpC (SKYSHYLADKMALQTSLYSVK EIARELAEIAYRRR)
TLR2 FACS	Miltenyi
α-mouse secondary antibody	Daco
α-rabbit secondary antibody	Daco

2.1.8 Standards

DNA ladder	Thermo Fisher GeneRuler 1kb
Protein ladder	Thermo Fisher PageRuler Plus Prestained

2.1.9 Primers

Table 2 List of primers

Name	Purpose	Sequence 5' – 3'
tcpC-H1-fwd	H1 forward, Exchange and Insert	CGAATATTGATTTCCCTTCC
tcpC-H1-Exchange-rev	H1 reverse & FLAG-tag	CTTGTCGTCATCGTCTTTGTAGTCTTGATGAAAAATTGCTTGTAA
Kan-Exchange fwd	Kanamycin cassette forward	GACGATGACGACAAGATTCCGGGGATCCGTCGAC
Kan-Exchange rev	Kanamycin cassette reverse	CGTATTATTGTGTGTAGGCTGGAGCTGCTTC
H2-Exchange-fwd	H2 forward	GCCAGCCTACACACAATAATACGCACTATGATTT
H2-Exchange-rev	H2 reverse	CATCATACCAAATAATTACACC
tcpC-H1-Insert-rev	H1 reverse & FLAG-tag	CTTGTCGTCATCGTCTTTGTAGTCCGTATTATTGTTATCTTGCATG
Kan-Insert-fwd	Kanamycin cassette forwards	CAAAGACGATGACGACAAGATTCCGGGGATCCGTCG
Kan-Insert -rev	Kanamycin cassette reverse	GGGATATGAAAAAATCATAGTGTGTAGGCTGGAGCTGCTTC
tcpC-H2-Insert-fwd	H2 forward	CACTATGATTTTTTCATATCCC
tcpC-H2-Insert-fwd	H2 reverse	TTAGGCCTAAATCAATATTTCTC
TcpC-into-pASK-fwd	TcpC + BsaI 5' overhang forwards	ATGGTAGGTCTCAGCGCCGTGATAGCATATGAAAACATAG
TcpC-into-pASK-rev	TcpC + BsaI 5' overhang reverse	ATGGTAGGTCTCATATCATCTTCTCCTGTATGCTATTTC
TcpCΔTIR-into-pASK-fwd	TcpC + BsaI 5' overhang forwards	ATGGTAGGTCTCAGCGCCGTGATAGCATATGAAAACATAG
TcpCΔTIR-into-pASK-rev	TcpCΔTIR + BsaI 5' overhang	ATGGTAGGTCTCATATCACGAAGTTCCTATACTTTCTAG

2.1.10 Plasmids

Table 3 List of plasmids

Plasmid	Description	Comments
pASK-IBA5plus	Anhydrotetracycline-inducible vector	Ampicillin resistance
pTcpC	pACYC184 containing TcpC Operon	Chloramphenicol resistance
pASK-TcpC	pASK-IBA5plus and full-length TcpC	Ampicillin resistance, inserted with BsaI
pASK-TcpCΔTIR	pASK-IBA5plus and amino acid 1-183 of TcpC	Ampicillin resistance, inserted with BsaI
pKD46	Vector enabling homologous recombination	Ampicillin resistance, heat-labile (incubate at 30°C)
pCP20	Vector encoding a flippase	Chloramphenicol resistance, heat-labile (incubate at 30°C)

2.1.11 Bacterial strains

CFT073	ATCC® 700928™
CFT073*ΔtcpC*	created by Andreas Wieser, Max von Pettenkofer-Institut, LMU München
CFT073*ΔtcpC*+pTcpC	CFT073 tcpC::kan complemented with pACYC184 TcpC Operon
CFT073+pASK-TcpC	CFT073 wild-type containing pASK-IBA5plus encoding TcpC
CFT073*ΔtcpC*+pASK-TcpC	CFT073*ΔtcpC* containing pASK-IBA5plus encoding TcpC
CFT073 FLAG-TcpC Insert	CFT073 with FLAG-tag inserted after position M163, created by me together with

	Silke Neumann-Pfeifer, nonsense mutation (G627T)
CFT073 FLAG-TcpC Exchange	CFT073 with FLAG-tag and FRT site exchanged with positions P155 – N166, created by me together with Silke Neumann-Pfeifer, nonsense mutation (T402C and G639T)
DH5α	Thermo Fisher

2.1.12 Cell lines

THP-1	ATCC TIB-202 ™
T24/83	bladder carcinoma cell line, kindly provided by Prof. Dr. Philipp Erben from Universitäts-medizin Mannheim

2.1.13 Software

GraphPad Prism	Statistical analysis
Magellan Spark	Cytokine measurements
Intas Gel Doc	analysis of agarose gels
Intas ChemoStar	development of western blots
FIJI	band density measurements
SerialCloner 2.6.1	primer design, cloning
CytExpert	FACS measurements
FlowJo	Analysis of FACS data

2.2 Methods

Molecular biology

2.2.1 Bacterial cultures

CFT073 and DH5α strains were cultured in LB medium at 37°C with shaking at 200 rpm. Strains containing plasmids were cultured using the appropriate antibiotic in the following concentrations unless stated otherwise: 100 µg/ml ampicillin, 50 µg/ml kanamycin, and 34 µg/ml chloramphenicol. Agar plates were prepared by dissolving 35 g/l Carl Roth LB Agar powder in ddH_2O. After autoclaving, the LB agar was cooled to room temperature, then heated in a microwave until liquefied before pouring into petri dishes, with the appropriate antibiotics added at this stage. Bacteria on agar plates were incubated at 37°C with the agar facing up.

2.2.2 DNA isolation

Plasmids were isolated from a 5 ml overnight culture. The cells in the culture were collected through three centrifugation steps at 11,000 x g for 30 seconds each in a 2 ml Eppendorf tube. Plasmids were isolated using the Macherey-Nagel NucleoSpin Plasmid Kit following the manufacturer's instructions. DNA was eluted in ddH2O for use in PCR or transformation.

2.2.3 Measurement of DNA concentration

DNA concentrations were measured with the NanoDrop using the accompanying nano volume cuvette and a 10x or 50x lid, depending on the concentration.

2.2.4 PCR

PCR reactions were performed with the Phusion DNA-Polymerase to ensure the best accuracy during cloning. The polymerase was used according to the manufacturer's instructions. Generally, an elongation time of 30 seconds per kilobase and 30 cycles were used in a 50µl reaction volume.

2.2.5 Gel electrophoresis and purification of PCR products

Agarose gels were prepared by heating 1% agarose in TAE buffer in a microwave until the liquid became clear. The mixture was cooled to approximately 50°C, and 10 µl

GelRed per 100 ml agarose solution was added and mixed thoroughly. The solution was poured into a mold, and an appropriate comb was inserted. The gel was allowed to cool until it solidified. The size of DNA fragments was determined by comparison to appropriate markers. Bands were visualized with UV light in a GelDoc.

To purify DNA fragments for cloning, bands were cut out from the agarose gels. In order to cut out the bands, the GelDoc was opened and the UV light was turned on while wearing eye gear providing UV protection. The visible bands were cut with a scalpel and transferred into 2 ml Eppendorf tubes. DNA from the cutouts was purified with the Macherey-Nagel Gel and PCR Clean-up Kit according to the manufacturer's instructions.

2.2.6 Restriction digestion

Restriction enzymes were used according to the manufacturer's instructions. Up to 1 µg DNA was digested in a 50 µl reaction at 37°C for 1 hour.

2.2.7 Cloning of plasmids

Plasmids were cloned using restriction cloning. Vector backbones were digested with suitable restriction enzymes to create a linear plasmid in which a DNA sequence of interest can be inserted. The vector was then purified in an agarose gel electrophoresis using the NucleoSpin Gel and PCR Clean-up Kit. The inserts were amplified with primers that produce a 5' overhang complementary to the restriction sites chosen in the vector. The amplified inserts were digested as described previously and purified directly using the NucleoSpin Gel and PCR Clean-up Kit. Afterwards, the purified inserts were ligated to the backbone using the Thermo Fisher Rapid DNA Ligation Kit and transformed into DH5α. Correct insertion of the desired sequences was confirmed by sequencing. The reading direction of all cloned inserts was 5' to 3'.

2.2.8 Transformation of plasmids into *E. coli*

Chemical transformation (DH5a)

During cloning, plasmids were transformed into *E. coli* DH5α via chemical transformation. Chemicompetent DH5α were prepared by diluting bacteria from a 5 ml

overnight culture 1:100 in an appropriate volume of LB medium. The bacteria were cultured until they reached an OD_{600} of 0.5, at which point the culture was cooled on ice for 30 minutes to stop further growth. The cells were then centrifuged at 2,500 x g for 5 minutes at 4°C. The supernatant was discarded, and the cells were washed three times in ice-cold 100 mM $CaCl_2$. After the final wash, the cells were resuspended in ice-cold 100 mM $CaCl_2$, 15% glycerol, and aliquoted in 100 µl. The aliquots were shock-frozen in liquid nitrogen and stored at -80°C.

Chemical transformation was performed by adding 10 – 100 ng plasmid DNA to an aliquot of chemocompetent DH5α and incubating on ice for 30 minutes. The cells were then heat-shocked at 42°C for 45 seconds, followed by a 2-minute incubation on ice. Next, 500 µl LB medium was added, and the cells were incubated at 37°C with shaking at 200 rpm for 1 hour. After incubation, the cells were centrifuged at 11,000 x g for 30 seconds, resuspended in 100 µl LB medium, and plated on LB agar plates containing appropriate antibiotics.

Electroporation (CFT073)

Plasmids were transformed into CFT073 strains via electroporation. Electrocompetent cells were prepared in the same way as chemocompetent cells; however, the cells were washed, resuspended, and aliquoted in 10% glycerol. Electroporation was performed with the Eppendorf Multiporator, and bacteria were pulsed once at 1500 V for 5 µs. Electroporation cuvettes with a 1 mm gap were used. After pulsing, 500 µl LB medium was added to the electroporation cuvette, mixed well with the bacteria, and transferred to a 1.5 ml Eppendorf tube. Bacteria were incubated at 37°C, 200 rpm for 1 hour, after which they were plated on LB agar plates containing appropriate antibiotics.

2.2.9 CFT073 FLAG-tag knock-in

The FLAG-tag was knocked into the TcpC gene of CFT073 through homologous recombination according to Datzenko & Wanner 2000. A PCR product was created with the following characteristics, going from 5’ to 3’. A homologous region to TcpC (H1), an FRT site, a kanamycin resistance cassette, another FRT site, the FLAG-tag sequence, and another homologous region to TcpC (H2).

The red helper plasmid pKD46 was transformed into wild-type CFT073 via electroporation. The plasmid is heat-labile; therefore, the transformed bacteria were incubated at 30°C for two days after plating on LB agar plates containing 100 µg/ml ampicillin. The expression of the proteins necessary for the homologous recombination process from pKD46 then had to be induced by L-arabinose. A 5 ml LB culture containing ampicillin was inoculated with a single colony and incubated overnight at 30°C, 200 rpm. The next day, a 500 ml LB culture containing ampicillin and 1 mM L-arabinose was inoculated with the 5 ml overnight culture and incubated at 30°C, 200 rpm until an OD_{600} of 0.6 was reached. From this culture, electrocompetent CFT073, ready for the homologous recombination, was produced as described before. Into these cells, 100 – 200 ng of the previously produced PCR product containing the FLAG-tag were transformed via electroporation. Immediately after electroporation, the cells were taken up in 1 ml SOC medium and incubated at 37°C with slight agitation for 1 hour. Cells were then plated on LB agar plates containing kanamycin at 37°C for 1 – 2 days. The incubation at 37°C also degrades the pKD46 plasmid, so it does not interfere with further treatment, for example, by providing ampicillin resistance. The correct insertion was then confirmed with colony PCR.

The inserted kanamycin resistance cassette has its own promoter and had to be removed in order not to interfere with the expression of the FLAG-tagged TcpC. The removal was facilitated by the inserted FRT sites and the plasmid pCP20 encoding an FLP recombinase. The plasmid pCP20 was transformed into FLAG-tagged CFT073 via electroporation. After transformation, the cells were taken up in 1 ml SOC medium and incubated at 30°C with slight agitation for 1 hour and then plated on LB agar plates containing 160 µg/ml chloramphenicol. pCP20 provides resistance to chloramphenicol, and after incubation at 30°C for 2 days, single colonies were picked, streaked onto a fresh LB agar plate without antibiotics, and incubated overnight at 42°C to degrade the pCP20 plasmid. Afterward, the growth of the CFT073 FLAG-TcpC strains was tested with ampicillin, kanamycin, and chloramphenicol. Colonies that did not grow on any antibiotic were selected to be sequenced.

2.2.10 Sequencing

Samples were sent to LGC Genomics for sequencing. The company was acquired by Eurofins Genomics as of 16.04.2025.

2.2.11 Protein expression in *E. coli*

Potassium stimulation of TcpC expression

CFT073 and CFT073*ΔtcpC* were incubated in 5 ml M9 minimal medium without potassium. The next day, the overnight culture was transferred to 20 ml of M5 minimal medium without potassium or 20 ml M9 minimal medium supplemented with 200 mM KCl and cultured for 4 hours. The bacteria were pelleted by centrifugation at 8000 x g for 5 minutes. Total cytoplasmic protein was extracted, protein concentration measured, and a western blot performed. TcpC was detected with our TcpC antibody. GAPDH was used as a loading control. The relative expression of TcpC was calculated with band densitometry using FIJI.

Overexpression in pASK-IBA5plus vector

Overnight cultures were diluted 1:50 in LB medium with the appropriate antibiotic and grown until reaching an OD_{600} of 0.5 in LB medium. To induce overexpression, anhydrotetracycline was added at specified concentrations for 1 – 3 hours. Then, bacteria were pelleted by centrifugation at 8000 x g for 5 minutes. The pellets were used to extract cytoplasmic proteins, or the supernatant was used for the detection of TcpC or for treating THP-1 monocytes.

2.2.12 Protein extraction and measurement of protein concentration

Cytoplasmic proteins from bacteria were extracted using a combination of heat and chemical lysis. Bacteria were pelleted by centrifugation at 8,000 x g for 5 minutes. The pellet was resuspended in TE buffer containing 1 mg/ml lysozyme and incubated at 37°C for 15 minutes. Next, an equal volume of 2x SDS lysis buffer was added, and the solution was incubated at 98°C for 15 minutes. After lysis, the solution was centrifuged at 16,000 x g for 15 minutes to remove cell debris. The supernatants were used to measure protein concentration and perform western blots. Eukaryotic cells were lysed with RIPA buffer. The cells were incubated for 30 minutes at 4°C on a rotator, followed by centrifugation at 16,000 x g for 15 minutes to remove cell debris. The supernatants were used to measure protein concentration and perform western blots.

The protein concentration was measured using the Bradford assay. To calculate the protein concentrations of the samples, a standard of BSA with known concentrations ranging from 1.5 – 0.09375 µg/ml was used. The samples were diluted 1:10 with ddH2O, and 5 µl of the sample was pipetted into a 96-well plate in triplicate. For each sample, 250 µl Bradford reagent was added, and the mixture was incubated for 10 minutes at RT. The absorbance of the samples was measured with the Tecan Spark 10M at 595 nm. The protein concentrations of the samples were automatically calculated by the measurement software Magellan Spark control using the BSA standards as a reference.

2.2.13 Production of TcpC in culture supernatants

Overnight cultures of CFT073, CFT073*ΔtcpC,* and CFT073*ΔtcpC*+pASK-IBA5plus-TcpC were diluted 1:100 in 20 or 60 ml LB medium and cultured until reaching an OD_{600} of 0.5. Afterwards, bacteria were washed three times with infection medium, and CFT073*ΔtcpC*+pASK-IBA5plus-TcpC cultures were either induced with specified amounts of anhydrotetracycline (Atc) or not induced. The cultures were then incubated for 3 hours at 37°C, 200 rpm. Bacteria were then centrifuged at 8000 x g for 5 min, and culture supernatants were filtered through a 0.2 µm syringe filter to clear the supernatants of residual bacterial bodies. The supernatants were concentrated 1:20 using an Amicon 10 kDa molecular weight cutoff (mwco) centrifugation filter. 15 ml supernatant was transferred to the Amicon filter at a time and centrifuged at 4000 x g for 10 minutes at RT in a fixed-angle centrifuge rotor. Afterwards, the flow-through was discarded and the Amicon filter was filled with the remaining volumes of each supernatant. This step was also used to wash the samples three times with fresh medium. The concentrated supernatants were stored at -20°C. For treatment of the cells, they were diluted 1:40 in infection medium.

2.2.14 Immunoprecipitation

Cells were lysed, and total protein concentration was measured as described earlier. 10 µl Protein-A agarose beads per sample were washed three times in ice-cold IP buffer by centrifugation at 3,200 x g for 30 seconds at 4°C. Approximately 150 µg total protein was added to the IP buffer with a final volume of 1 ml and precleared with washed protein-A agarose beads for 1 hour at 4°C on a disc rotator. After 1 hour, the

samples were centrifuged at 3,200 x g for 30 seconds at 4°C to pellet the agarose beads. The supernatants were carefully transferred to new Eppendorf tubes with a 200 µl pipette. At this point, 1 µg of primary antibody targeting the protein to be immunoprecipitated was added and incubated for 2 hours at 4°C on a disc rotator. 10 µl Protein-A agarose beads per sample were washed three times in ice-cold IP buffer by centrifugation at 3,200 x g for 30 seconds at 4°C, added to the samples, and incubated overnight at 4°C on a disc rotator. The next day, the samples were centrifuged at 3,200 x g for 30 seconds at 4 °C. The supernatant was carefully aspirated with a 200 µl pipette, and the samples were washed three times with 500 µl ice-cold IP buffer as described before. After the last washing step, the supernatant was aspirated and a 10 ml pipette with a flattened tip was used to aspirate as much IP buffer as possible. 2x Laemmli buffer was added to the agarose beads, and the samples were boiled at 98°C for 5 minutes to release the precipitated proteins from the beads. The IP input and eluate of the samples were then analyzed with a western blot.

2.2.15 SDS-PAGE

For the SDS-PAGE, 12% polyacrylamide was used in the resolving gel and 4% polyacrylamide was used in the stacking gel. The resolving gel was poured first, then overlaid with isopropanol to remove air bubbles and ensure a straight edge after polymerization. After polymerization of the resolving gel, the stacking gel was added on top, and a comb with an appropriate number of wells was inserted. 1 mm spacers were used to cast the gels, and they were stored in a humid environment at 4°C for up to 7 days.

Samples were mixed with Laemmli buffer and boiled at 98°C for 5 minutes. The gels were run in a Bio-Rad system at 80 V for 20 minutes, followed by 150 V until the loading dye ran off the gel. PageRuler Plus Prestained Protein Ladder was used as a marker.

2.2.16 Western Blot

<u>Wet blot</u>

The polyacrylamide gel, a nitrocellulose membrane (pore size 0.2 µm), and two filter papers were equilibrated in western blot transfer buffer for 5 minutes. The equilibrated polyacrylamide gel was placed on the nitrocellulose membrane and sandwiched

between two filter papers. The sandwich was placed in the tank so that the proteins migrated toward the anode onto the nitrocellulose membrane. The blot was run at 100 V for 2 hours.

Semi-dry blot

Semi-dry western blots were performed with the Trans-Blot Turbo Transfer System from Bio-Rad with the preset programs. The polyacrylamide gel, a nitrocellulose membrane (pore size 0.2 µm), and two filter papers were equilibrated in Towbin transfer buffer for 5 minutes. The equilibrated polyacrylamide gel was placed on top of the nitrocellulose membrane and sandwiched between two filter papers. This sandwich was placed into the cassette. One gel was run with the MINI program, and two gels were run with the MIDI program.

After transfer, the nitrocellulose membranes were washed three times for 5 minutes each in TBS-T, followed by blocking for 1 hour in TBS-T + 5% non-fat milk powder at RT and slight agitation. The membranes were then washed three times for 5 minutes each in TBS-T. Primary antibodies were diluted 1:1,000 in TBS-T + 3% non-fat milk powder, and the membranes were either incubated overnight at 4°C or for 1 hour at RT with slight agitation. The membranes were washed again as described before and then incubated with the secondary antibody, diluted 1:3,000 in TBS-T + 3% non-fat milk powder, for 1 hour at RT with slight agitation. After another wash, the membranes were developed using a Chemi-Doc system. The software automatically adjusted the contrast, and the resulting images were exported from the program.

2.2.17 ELISA

Cytokines from culture supernatants were measured using the ELISA DuoKit by R&D Systems according to the manufacturer's instructions. Measurements were performed with a Tecan Spark 10M. The cytokine concentrations of the samples were calculated using the measurement software Magellan Spark with the standards provided in the ELISA kits.

Cell biology

2.2.18 Cell culture

THP-1 cells, PBMCs, primary monocytes, and MDMs were cultured in RPMI 1640 supplemented with 10% FCS. THP-1 cells were split 2 – 3 times a week and maintained in culture for about 4 weeks. T24/83 cells were cultured in McCoy's 5A medium with 10% FCS. They were split or used for experiments when approximately 80 – 90% confluency was reached. All eukaryotic cells were incubated at 37°C with 5% CO_2. The cells were treated with Trypan blue, and living cells were counted using a Neubauer hemocytometer.

2.2.19 Isolation of PBMCs and peripheral blood monocytes

PBMCs were isolated from buffy coats of healthy donors using density centrifugation. Buffy coats were diluted 1:3 with PBS. Then, 15 ml BioColl (1077 g/ml) was carefully overlayed with 30 ml diluted buffy coat, avoiding mixing of the phases, and centrifuged at 400 x g, RT for 30 minutes in a swing-bucket rotor without brakes. After centrifugation, PBMCs were carefully transferred to a 50 ml Falcon tube with a pipette. PBMCs were washed with 30 ml PBS and centrifuged at 300 x g for 10 minutes until the supernatant was clear.

The cells were then counted and centrifuged again at 300 x g for 10 minutes. The supernatant was discarded, and the pellet was resuspended in 80 µl MACS buffer (PBS, 2 mM EDTA, 0.5% BSA) per 10^7 cells. Next, 20 µl CD14 microbeads per 10^7 cells were added and mixed thoroughly. The PBMCs and CD14 microbeads were incubated for 15 minutes in the refrigerator. The cells were washed with 1 – 2 ml MACS buffer per 10^7 cells and centrifuged at 300 x g for 10 minutes. The supernatant was discarded, and the pellet was resuspended in 500 µl MACS buffer per $5x10^7$ cells. MS columns were placed in the MACS separator and rinsed with 500 µl MACS buffer. After rinsing, 500 µl cell suspension was loaded into the column. Once all the liquid had passed through, the columns were washed three times with 500 µl MACS buffer. The columns were then removed from the magnetic separator and placed in a 15 ml Falcon tube. Finally, 1 ml MACS buffer was pipetted into each column, and the labeled cells were flushed out by pushing the plunger into the column. The cells were then counted, and they were put into culture. The purity of the peripheral blood monocytes was confirmed with FACS analysis according to Nielsen, et al., 2020. Generally, a purity of more than 90% was achieved.

2.2.20 Differentiation of monocytes into macrophages

Human peripheral blood monocytes were differentiated into MDMs in culture medium supplemented with 10 ng/ml M-CSF and 1 ng/ml GM-CSF for 6 days. The medium was changed every 2 – 3 days.

2.2.21 Infection of eukaryotic cells with *E. coli*

The day before the infection, overnight cultures of CFT073, CFT073*ΔtcpC*, and CFT073*ΔtcpC*+pTcpC were prepared.

On the day of the infection experiment, monocytes were transferred from T125 flasks into 50 ml Falcon tubes and washed three times with 10 ml infection medium by centrifugation at 300 x g for 10 minutes at RT. After washing $4x10^5$ cells per well were seeded in a volume of 500 µl into 24-well plates. The plates were placed in the incubator until the bacteria were prepared.

$4x10^5$ Macrophages were seeded in 24-well plates before differentiation, and T24/83 cells were seeded in 24-well plates one day before the infection. Since both cell types are adherent, they were washed three times with 1 ml infection medium on the day of the infection experiment inside the 24-well plates and placed into the incubator until the bacteria were prepared.

The bacterial overnight cultures were also washed three times in 5 ml infection medium by centrifugation at 8000 x g for 5 minutes at 4°C to stop growth during preparation. After washing, the overnight cultures of the three strains were diluted to an OD_{600} of 0.5 in a 50 ml Falcon tube. From this suspension, the bacteria were diluted to the appropriate MOIs in a serial dilution where the concentration was calculated per 500 µl. 500 µl of bacteria suspension was added to each of the corresponding wells for a total volume of 1 ml during the infections. As a positive control, 100 ng/ml LPS was used. Only infection medium was used the negative control. Each condition was prepared in triplicate. The plates were then incubated at 37°C with 5% CO_2 for 5 hours. After 4 hours, 5 mM ATP was added to the LPS/positive control to activate the NLRP3 inflammasome and release IL-1β. After 5 hours of infection, 400 µl supernatant was collected from each sample and frozen at -20°C until further use.

Additionally, from each strain, samples were diluted 1:500,000 to be plated on LB agar plates as a control of the OD_{600} measurement. 100 µl of the dilution was plated on 3 – 6 LB agar plates per strain. They were placed in an incubator and counted on the next day.

2.2.22 Invasion of CFT073 into T24/83 cells

One day before the experiment, $4x10^5$ cells per well were seeded in a flat-bottom 24-well plate in complete culture medium. On the following day, the cells were washed three times with infection medium. Afterwards, CFT073, CFT073*ΔtcpC*, and CFT073*ΔtcpC*+pTcpC were added at an MOI of 50 to the wells containing T24/83 cells. As a negative control, only infection medium was added to the cells. Each condition was prepared in triplicate. The plates were then centrifuged at 100 x g for 10 minutes to facilitate contact between bacteria and the T24/83 cells. The plates were incubated for 1 hour to allow bacterial invasion of the T24/83 cells. After one hour, the supernatant was carefully aspirated, and the cells were washed three times with PBS. Infection medium supplemented with 400 µg/ml gentamicin was added for 3 hours to kill all extracellular bacteria. The cells were then carefully washed again, and 1 ml of 1% Saponin was added and incubated for 10 minutes at RT. Each well was mixed thoroughly by pipetting up and down to detach all cells from the bottom of the well, then transferred to a 1.5 ml Eppendorf tube. Each tube was briefly vortexed on the highest setting and diluted 1:200 with PBS. From each well, 100 µl was plated onto an LB agar plate. To confirm that gentamicin killed the extracellular bacteria, 100 µl supernatant from six wells was also plated on LB agar plates.

2.2.23 Treatment of THP-1 cells with conditioned medium and LPS plus ATP

THP-1 monocytes were washed three times in infection medium, and $4x10^5$ cells per well were seeded in 400 µl infection medium in 24-well plates. To each well, 100 µl LPS with a concentration of 1 µg/ml was added to reach a final working concentration of 100 ng/ml. The concentrated culture supernatants of CFT073, CFT073*ΔtcpC*, and CFT073*ΔtcpC*+pASK-IBA5plus were diluted to 1:1, and 500 µl were transferred to the corresponding wells. THP-1 cells treated with only 100 ng/ml LPS or infection medium served as positive and negative controls, respectively. After 2 hours 5 µM ATP was

added to the samples and the positive control to stimulate IL-1β release. The plates were incubated for a total of 3 hours at 37°C and 5% CO_2 after which, 400 µl culture supernatants were collected for analysis of released cytokines. Samples were stored at -20°C until further use.

3 Results

3.1 TcpC modulates the immune response of peripheral blood cells

It has already been reported that TcpC inhibits the release of the proinflammatory cytokines TNFα and IL-1β in bone marrow-derived macrophages (BMDMs) and the mouse macrophage cell line RAW267.4, respectively, during an infection of these cells with CFT073. However, infections with bone marrow-derived dendritic cells show that besides an inhibitory effect, there seem to be conditions in which TcpC is able to stimulate the release of proinflammatory cytokines. I now wanted to explore this dichotomy and whether human cells show the same immune response. Experiments leading to my project already showed that human cells react quite differently to an infection of CFT073, CFT073*ΔtcpC,* and CFT073*ΔtcpC*+pTcpC. The infection of the human monocyte cell line THP-1 with the strains mentioned above led to increased release of the proinflammatory cytokines IL-1β and TNFα in the presence of TcpC. The differentiation of THP-1 monocytes into macrophages using PMA abrogated the stimulatory effect of TcpC on cytokine release.

My first goal was to validate these findings with primary human cells. In order to do that, I isolated PBMCs, peripheral blood monocytes from buffy coats obtained from healthy donors, and differentiated the monocytes into MDMs.

Infections of the PBMCs show that TcpC significantly stimulates the release of proinflammatory cytokines IL-1β (Fig. 2 A, C, E) and TNFα (Fig. 2 B, D, F), however, in a donor-dependent manner. The bacterial load is also an important factor. At MOI 1, I can detect almost no cytokines, indicating that the bacterial load is too high for the PBMCs for a proper immune response. The cytokine release of the PBMCs increases when lowering the MOI to 0.1 or 0.01 where I start seeing a TcpC-dependent phenotype. I infected PBMCs from six different donors, of which three are depicted here. They generally show the stimulatory effect of TcpC, however, there are donor-dependent differences.

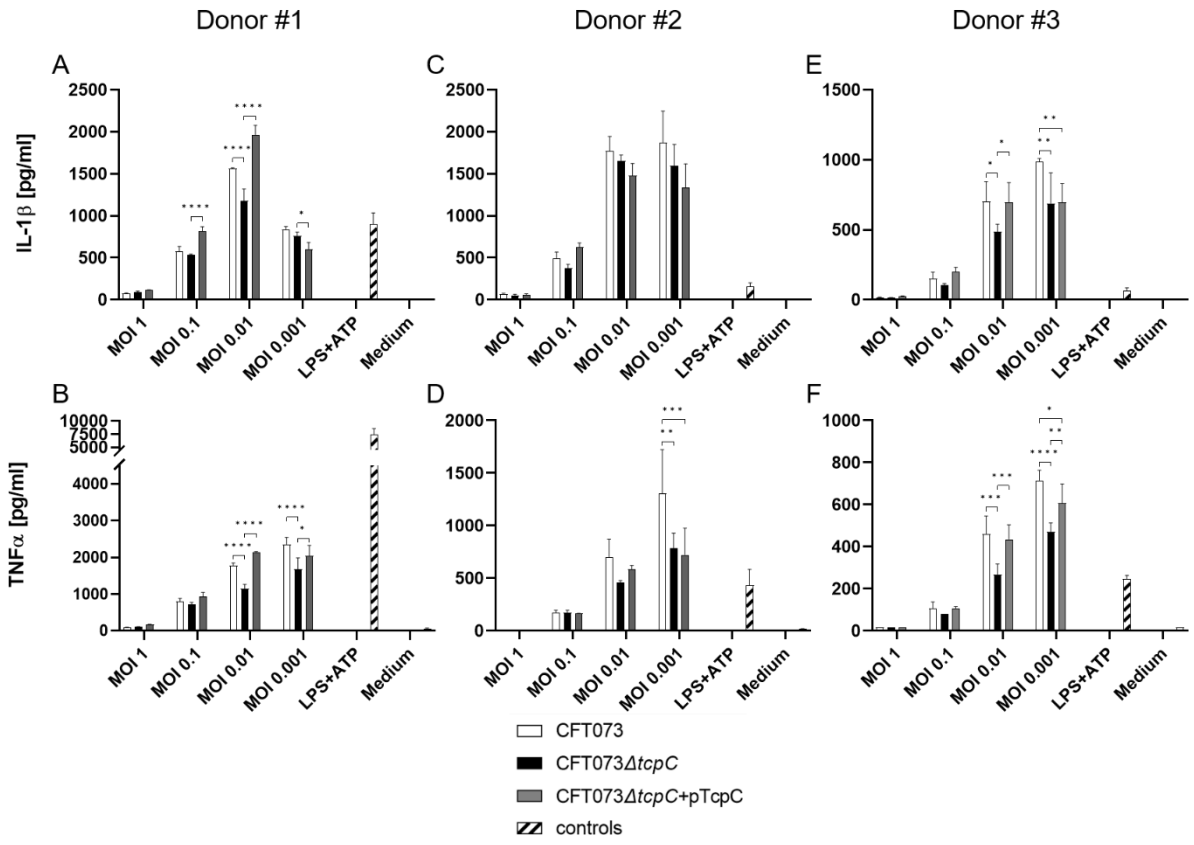

Figure 2 TcpC stimulates release of proinflammatory cytokines of PBMCs.

PBMCs were obtained by density centrifugation of diluted buffy coats obtained from healthy donors. PBMCs were infected with the indicated MOIs for 5 hours, after which culture supernatants were collected and cytokine release of the PBMCs was measured with ELISA. Stimulation with 100 ng/ml LPS with the addition of 5 µM ATP, 4 hours post-infection, served as a positive control, and treatment with infection medium served as a negative control. The graphs show the mean and SD of 3 of 6 independent donors performed in triplicate. Statistical analysis was done by 2-way ANOVA and post-hoc Tukey test using GraphPad Prism.

PBMCs are a mixture of several peripheral blood immune cells, including B and T lymphocytes, NK cells, dendritic cells, and monocytes. In the early response to urinary tract infections, the most important cells of the PBMCs are the monocytes, since they migrate to the infection site shortly after the neutrophils, where they promote inflammation and differentiate into macrophages in order to phagocytose the bacteria. To investigate the effect of TcpC on peripheral blood monocytes during an infection, I isolated them from the PBMCs. The infection of the peripheral blood monocytes with TcpC-producing CFT073 caused an increased release of the proinflammatory cytokines IL-1β (Fig. 3 A, C, E) and TNFα (Fig. 3 B, D, F) compared to the infection with the TcpC knockout mutant. When complementing the TcpC knockout mutant with the low-copy plasmid pACYC184 encoding TcpC, the stimulatory ability can be

restored to similar levels as those of CFT073 wild-type. This confirms the data obtained by my colleague in the THP-1 cell line, where I could observe the same stimulatory effect of TcpC. However, the response of the peripheral blood monocytes to the infection is more heterogeneous and more donor-dependent. That is to be expected as peripheral blood cells represent the donors individual immune system, whereas the THP-1 cell line is derived from one donor. These findings indicate that TcpC is involved in producing a stronger proinflammatory response upon infection. I infected peripheral blood monocytes from six different donors, of which three are depicted here. They all show the stimulatory effect of TcpC.

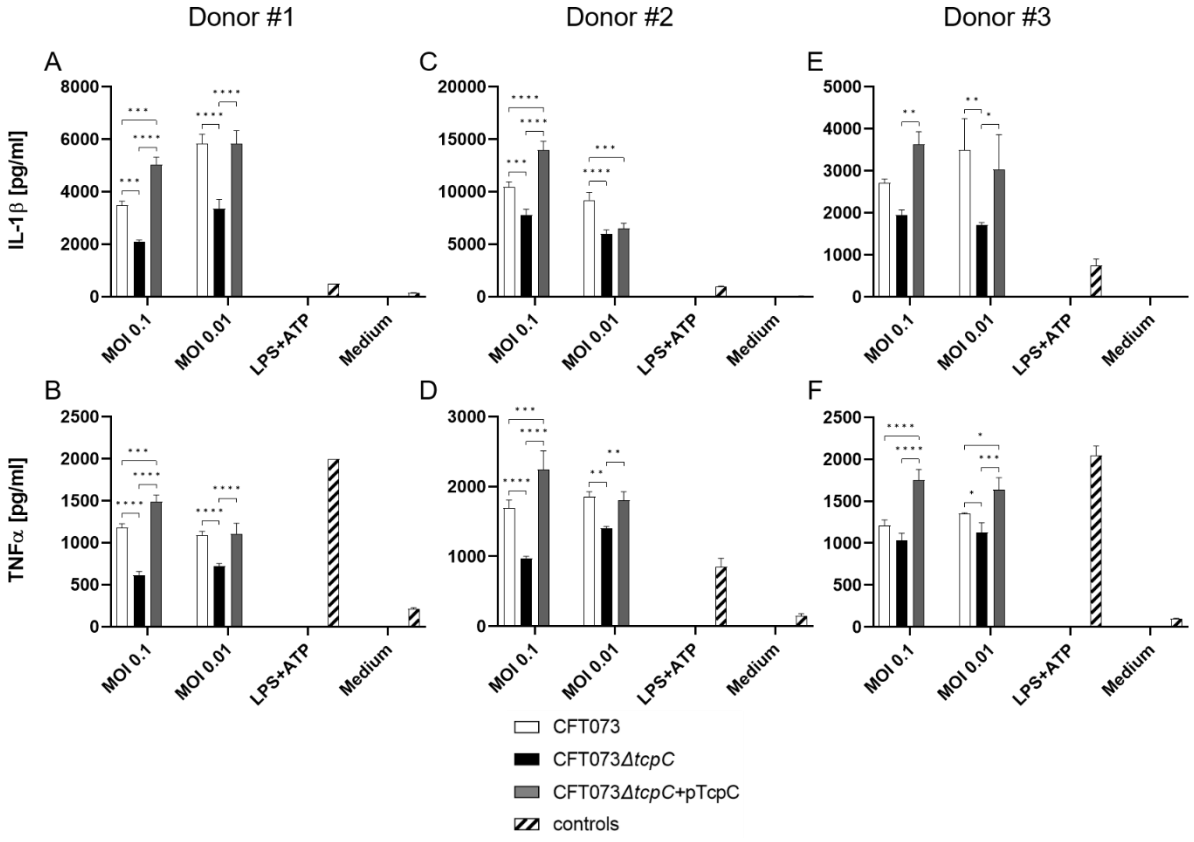

Figure 3 TcpC stimulates release of proinflammatory cytokines of peripheral blood monocytes.

Peripheral blood monocytes were obtained by positive selection from PBMCs with CD14 microbeads. The monocytes were infected with the indicated MOIs for 5 hours, after which culture supernatants were collected and cytokine release of the monocytes was measured with ELISA. Stimulation with 100 ng/ml LPS with the addition of 5 µM ATP, 4 hours post-infection, served as a positive control, and treatment with the infection medium served as a negative control. The graphs show the mean and SD of 3 of 6 independent donors performed in triplicate. Statistical analysis was done by 2-way ANOVA and post-hoc Tukey test using GraphPad Prism.

Experiments leading to my project showed that the differentiation of THP-1 monocytes into macrophages caused an overall stronger response, represented in higher amounts of released cytokines, and completely abrogated the stimulatory effect of TcpC on the release of IL-1β. The differentiation of the peripheral blood monocytes into MDMs causes an approximately 20 times stronger TNFα response, but contrary to THP-1 cells, the IL-1β response is roughly the same between monocytes and macrophages. MDMs also show a reduction of the TcpC-dependent stimulation of cytokine release, but do not completely abrogate it. At the lower MOI of 0.01, I can see no difference in IL-1β release (Fig. 4 A, C, E) between the different CFT073 strains anymore, but the MDMs still show a trend of TcpC-dependent stimulation of TNFα release across both MOIs (Fig. 4 B, D, F).

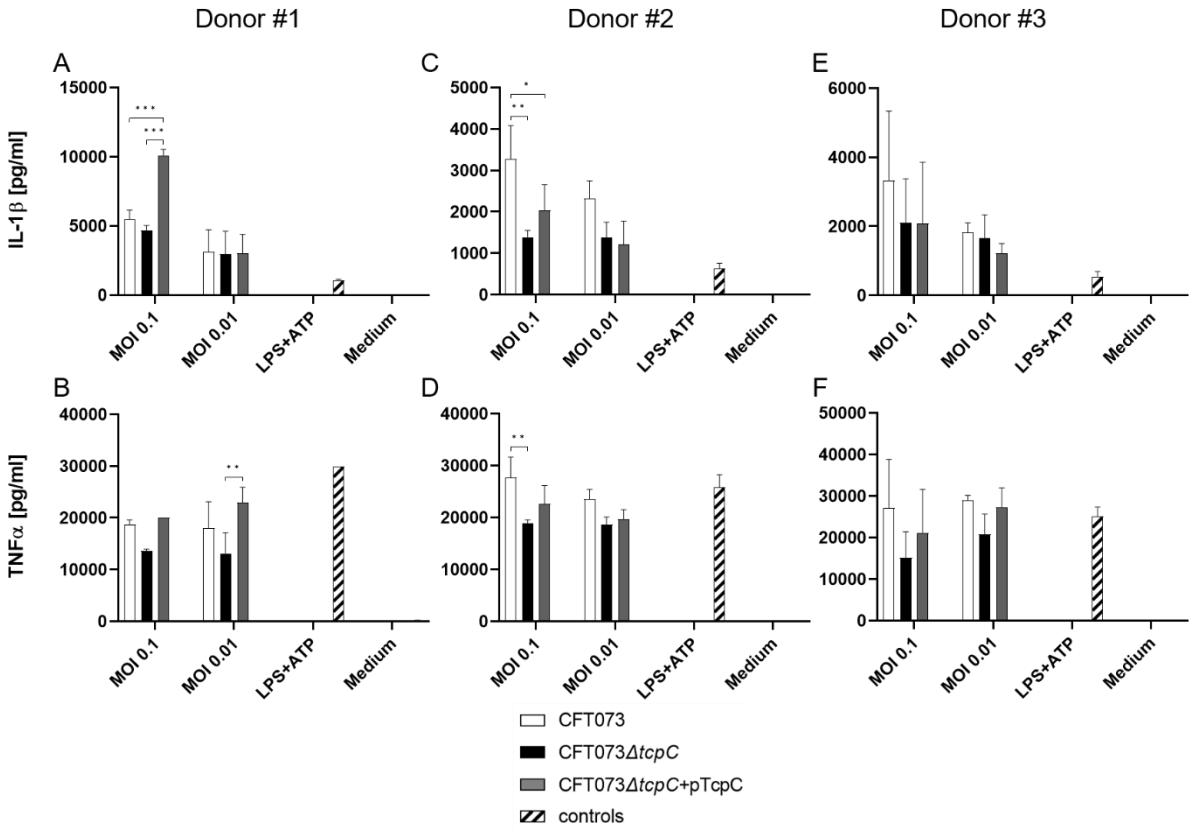

Figure 4 Differentiation into macrophages reduces stimulation by TcpC.

Monocyte-derived macrophages were obtained by differentiation of peripheral blood monocytes with M-CSF and GM-CSF. The MDMs were infected with the indicated MOIs for 5 hours, after which culture supernatants were collected and cytokine release of the MDMs was measured with ELISA. Stimulation with 100 ng/ml LPS with the addition of 5 µM ATP, 4 hours post-infection, served as a positive control, and treatment with the infection medium served as a negative control. The graphs show the mean and SD of 3 independent donors performed in triplicate. Statistical analysis was done by 2-way ANOVA and post-hoc Tukey test using GraphPad Prism.

3.2 TcpC stimulates cytokine release of bladder cells

In order to further investigate the proinflammatory effect of TcpC during UTIs I decided to include another cell type. Besides monocytes and macrophages, neutrophils and bladder epithelial cells are the earliest responders to a UTI. When bacteria reach the bladder, bladder epithelial cells are the first cells to respond, releasing cytokines to attract immune cells and start the proinflammatory response. For that reason, I decided to additionally infect the bladder carcinoma cell line T24/83 with CFT073, CFT073*ΔtcpC*, and CFT073*ΔtcpC*+pTcpC. T24/83 infected with CFT073 and CFT073*ΔtcpC*+pTcpC release an increased amount of the proinflammatory cytokines TNFα (Fig. 5 A) and IL-6 (Fig. 5 B), demonstrating that the ability of TcpC to stimulate a proinflammatory response is not unique to monocytes but applies to other cells involved in the early response to a UTI.

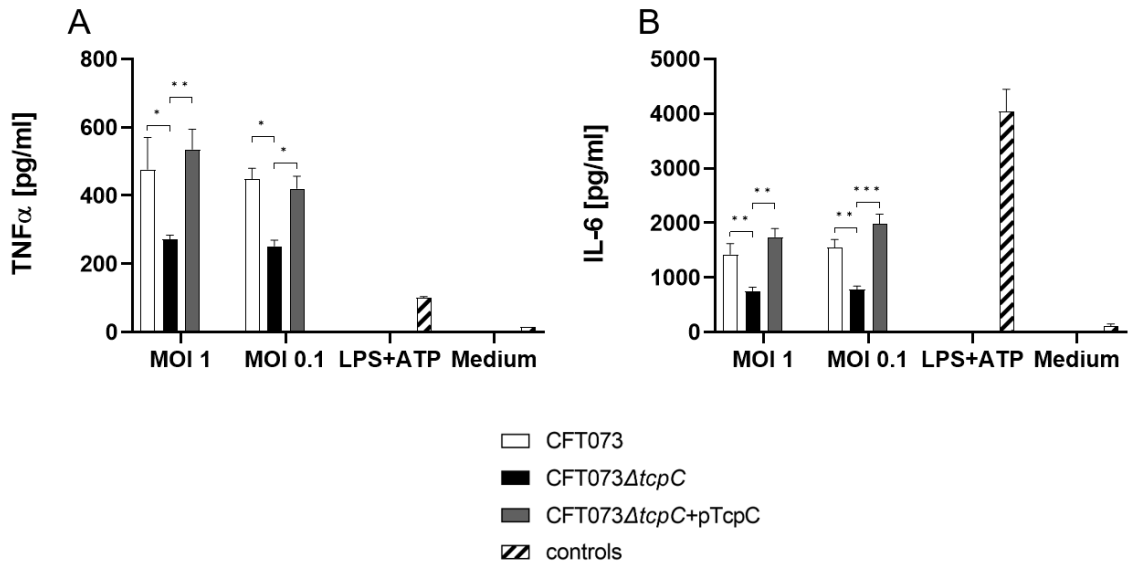

Figure 5 TcpC stimulates the release of proinflammatory cytokines in T24/83 cells.

T24/83 cells were infected with the indicated MOIs for 5 hours, after which culture supernatants were collected and cytokine release of the cells was measured with ELISA. Stimulation with 100 ng/ml LPS plus ATP served as a positive control, and treatment with the infection medium served as a negative control. Statistical analysis was done by 2-way ANOVA and post-hoc Tukey test using GraphPad Prism. Data is shown as mean and SEM from two independent experiments.

Another reason why I chose this cell line was that we have mutants of T24/83 in which TLR4 or MyD88 were knocked out via CRISPR-Cas9 gene editing by two colleagues of mine. It allowed me to investigate where TcpC might modulate the immune response to CFT073.

The MyD88-deficient T24/83 cells exhibited a generally weaker response to bacterial and LPS plus ATP stimulation, as indicated by reduced release of TNFα and IL-6. LPS plus ATP stimulation was not able to elicit a measurable TNFα response, and the response to the CFT073 strains was roughly four times lower at MOI 0.1 and more than four times lower at MOI 1 compared to infected T24/83 wild-type cells (Fig. 6 A). The IL-6 response was also lower compared to the response of T24/83, but surprisingly, the cells still exhibited a substantial IL-6 response after LPS plus ATP stimulation (Fig. 6 B). The reduction in cytokine release was to be expected since the MyD88-deficient cells are missing a vital adapter protein of TLR4, interfering with the MyD88-dependent signaling. However, the TcpC-dependent stimulation of cytokine release persists. It suggests that TcpC can affect TLR4 signaling independent of MyD88.

The knockout of TLR4 shows that without the receptor, the cells are not able to respond with TNFα release to the infection with CFT073 or the stimulation with LPS plus ATP (Fig. 6 C). Similar to the MyD88-deficient cells, a TLR4 deficiency leads to a reduction in IL-6 release upon infection and LPS plus ATP stimulation, although both LPS plus ATP stimulation and the infection with bacteria still lead to a slight increase in IL-6 release (Fig. 6 D) compared to the negative control. However, in contrast to the deficiency of MyD88, a TLR4 deficiency completely abrogates the stimulatory effect of TcpC. This demonstrates that without the activation of TLR4, TcpC cannot stimulate a proinflammatory response, and the bacteria have to be recognized by TLR4. It also suggests that TcpC modulates the immune response of these cells downstream of the recognition.

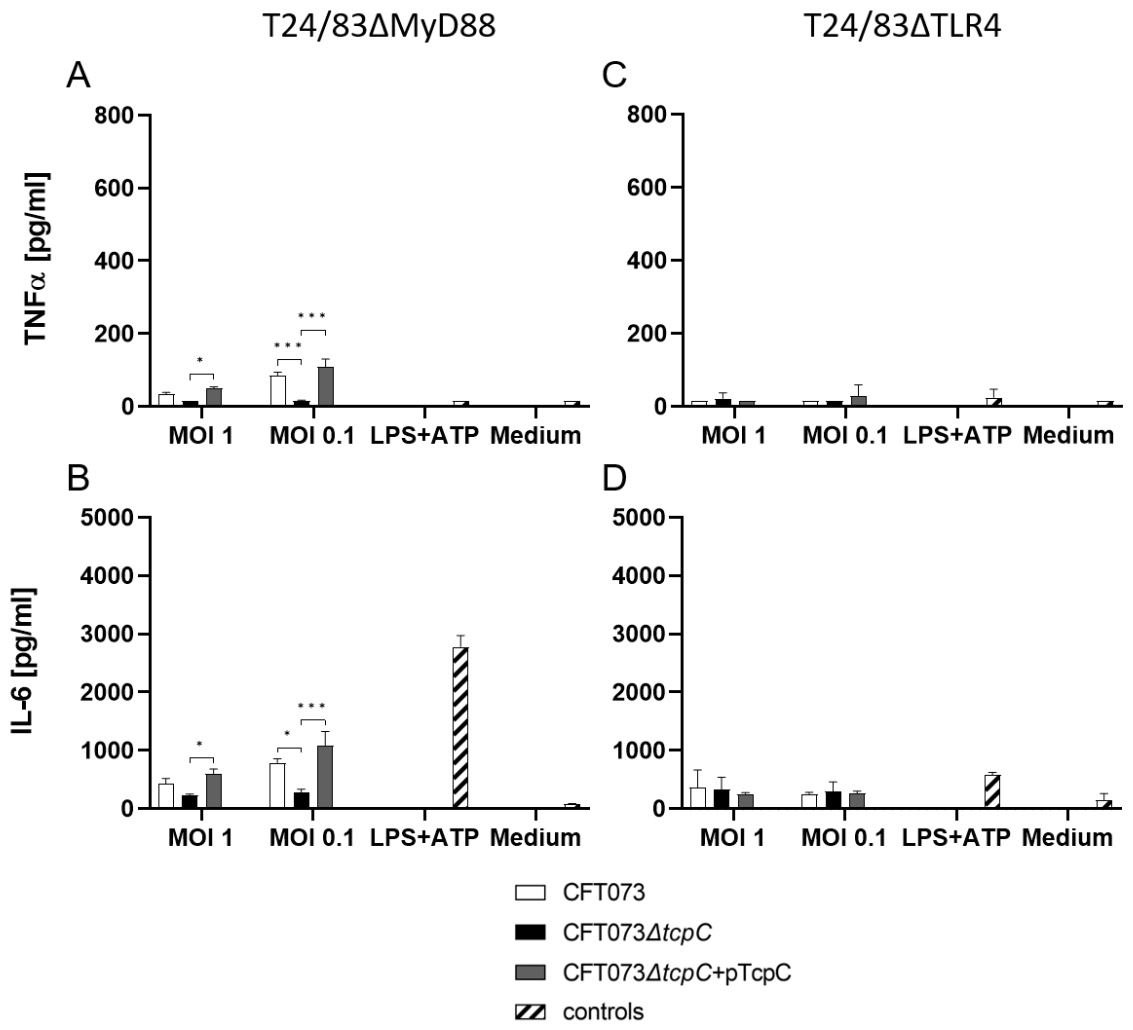

Figure 6 Recognition by TLR4 is needed for TcpC to stimulate the release of proinflammatory cytokines.

T24/83 mutants were infected with the indicated MOIs for 5 hours, after which culture supernatants were collected and cytokine release of the cells was measured with ELISA. Stimulation with 100 ng/ml LPS plus ATP served as a positive control, and treatment with the infection medium served as a negative control. Statistical analysis was done by 2-way ANOVA and post-hoc Tukey test using GraphPad Prism. Data is shown as mean and SEM from two independent experiments.

3.3 TcpC does not promote invasion into bladder cells

One hallmark of uropathogenic *E. coli* during UTIs is the invasion of bladder epithelial cells. The increase in bacteria that encode TcpC can be observed during disease progression from cystitis to pyelonephritis, and the formation of kidney abscesses during pyelonephritis in mice infected with TcpC-producing CFT073 indicates a correlation between TcpC and disease severity. Additionally, Yadav, et al. demonstrated that the C57BL/6 mice infected with CFT073 had higher bacterial numbers in the urine and the kidneys compared to mice infected with a TcpC knockout

mutant, both 4 and 7 days after infection. One reason for that could be that due to TcpC expression, CFT073 is able to better persist in the urinary tract by invasion of bladder epithelial cells and therefore evasion of the innate immune response. I wanted to address this by investigating the possibility of TcpC promoting invasion of CFT073 into T24/83 cells.

After an infection of T24/83 wild-type, the MyD88- and TLR4-deficient cells with an MOI of 50 for 1 hour, the extracellular bacteria were killed with a gentamicin treatment. Lysis of the cells and plating of their contents showed that the three CFT073 strains invaded approximately half of the T24/83 cells, assuming one bacterium per cell (Fig. 7). The infection of the TLR4-deficient cells shows a similar number, although the CFT073 strains seem to invade or persist in the cells slightly better. A deficiency of MyD88, on the other hand, noticeably but not statistically significantly reduced the ability of the CFT073 to invade the T24/83. This suggests that MyD88 may be involved in the uptake of the bacteria.

I cannot see a difference in the ability of CFT073 to invade T24/83 cells depending on TcpC. These results make it unlikely that TcpC helps persistence of CFT073 in the urinary tract by promoting invasion of epithelial tissues.

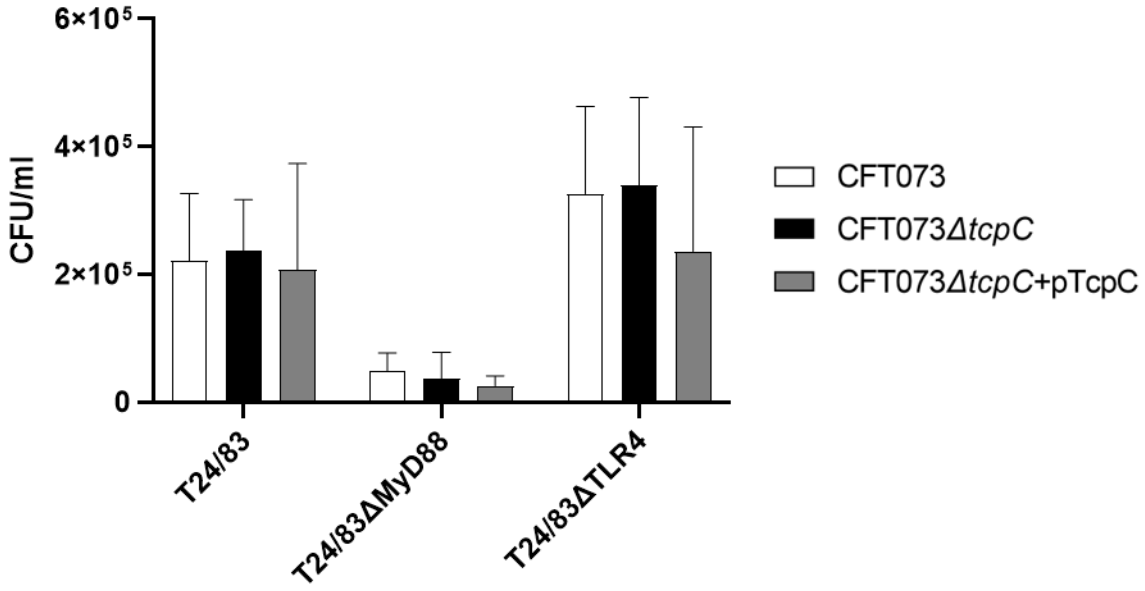

Figure 7 TcpC does not promote invasion of CFT073 into T24/83 cells.

T24/83 wild-type, ΔMyD88, and ΔTLR4 were infected with the indicated strain at an MOI of 50 for 1 hour. Afterwards, the cells were treated with 400 µg/ml gentamicin for 3 hours. The cells were then lysed in 1% saponin, plated on LB agar plates, and incubated overnight. The graphs represent the mean and SEM of three independent experiments.

3.4 Detection of TcpC

To perform functional studies with TcpC, it is imperative to detect the protein reliably. A peptide antibody was developed by immunization of rabbits against an amino acid sequence at the C-terminus of TcpC by the company Davids Biotechnologie (for reference see 2.1.7). My colleague, Dr. Silke Neumann-Pfeifer, purified the peptide used for immunization and ordered the production of the antibody. However, she was unsure whether the antibody was able to detect endogenous TcpC of CFT073 reliably. The antibody worked fine against TcpC overexpressed in *E. coli*. I decided to try detecting TcpC with an immunoprecipitation, and in order to confirm our TcpC antibody, and not use the same antibody for immunoprecipitation and detection. I chose to knock in a FLAG-tag into the TcpC gene of CFT073 wild-type. TcpC has two potentially important domains at the N-terminus and the C-terminus. The protein has an annotated transmembrane domain at the N-terminus. At the C-terminus, TcpC has an amino acid sequence similar to cell-penetrating peptide sequences that are described to be important for the uptake of TcpC into eukaryotic cells (Pasi, et al.,

2016). I did not want to interfere with these domains by adding a tag, which is why I decided to add the FLAG-tag in the middle of TcpC in front of the TIR domain. The idea was to preserve the endogenous function of TcpC in case the TcpC antibody was indeed not able to detect endogenous TcpC. By preserving its function, I would be able to use FLAG-tagged CFT073 in infections and use the FLAG antibody to detect TcpC. I added the FLAG-tag in two different approaches; one approach was simply adding the FLAG-tag after M163 of TcpC (CFT073 FLAG-TcpC Insert), and the second approach was to exchange the FLAG-tag with a short amino acid sequence at the positions P155 – N166 (CFT073 FLAG-TcpC Exchange). Sequencing of both mutated strains revealed two point mutations in CFT073 FLAG-TcpC Exchange, T402C and G639T, and one point mutation in CFT073 FLAG-TcpC Insert, G627T. However, the point mutations do not influence the amino acid sequence of the expressed TcpC. Therefore, I continued working with them.

In order to confirm the validity of our TcpC antibody, I performed an immunoprecipitation with the TcpC antibody and detected it with the TcpC antibody. Additionally, I performed the immunoprecipitation with the FLAG antibody and detected it with the TcpC antibody. TcpC has a size of approximately 36 kDa. Both immunoprecipitations show a protein that is detected at around 35 kDa, which corresponds to the size of TcpC (Fig. 8). Since both immunoprecipitations show a protein at the same size, I conclude that our TcpC antibody is working and suitable to detect TcpC not only from overexpression but also from endogenous expression. The size difference between the three samples is the result of the cloning strategies. In the CFT073 FLAG-TcpC Exchange strain, an amino acid sequence of 12 amino acids was removed and replaced by the FLAG-tag and the FRT site that is left as a scar after the removal of the kanamycin resistance cassette, which is 36 amino acids. That should lead to an approximate mass increase of 2.5 kDa. The mass of this protein should best represent the mass of the endogenous TcpC. In the CFT073 FLAG-TcpC Insert strain, the FLAG-tag and FRT site are inserted into TcpC, resulting in approximately 4 kDa more mass compared to the wild-type and FLAG-tag Exchange. The pASK-IBA5plus vector encodes a C-terminal strep-tag resulting in slightly more mass compared to FLAG-tag Exchange. Our TcpC antibody is able to detect TcpC in all three fractions: the pellet, the input, and the eluate (Fig. 8). The detection of a protein after immunoprecipitation with the FLAG antibody that has the same size as in the pellet and the input suggests that our antibody is capable of detecting TcpC. It is further

supported by the inability of the antibody to detect anything in the total protein from CFT073*ΔtcpC*.

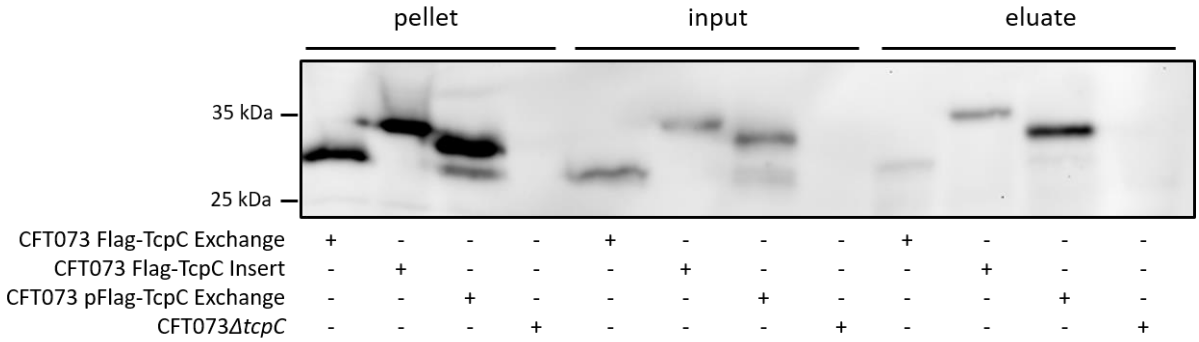

Figure 8 FLAG-tagged TcpC can be precipitated via FLAG antibody.

20 ml LB medium was inoculated with an overnight culture of CFT073 strains in a 1:100 dilution. The cultures were then incubated at 37°C, 200 rpm for 3 hours, after which the bacteria were pelleted by centrifugation. The cells were lysed using lysozyme, SDS lysis buffer, and heat. CFT073 wildtype with FLAG-tagged TcpC encoded on pASK-IBA5plus served as a positive control, and CFT073*ΔtcpC* served as a negative control. The pellet fraction represents proteins that were not in solution after lysis, the input fraction represents proteins in solution before immunoprecipitation, and the eluate represents proteins precipitated from the input with the FLAG antibody. The samples were run on a 12% SDS gel and visualized with our TcpC primary antibody.

However, since wild-type TcpC has no target for the FLAG antibody, I was not able to precipitate TcpC from CFT073 wild-type. In order to make sure that it is actually TcpC and I can detect endogenous TcpC from CFT073, I continued with an immunoprecipitation using our TcpC antibody. Here, I can show that our TcpC antibody precipitates a protein of a similar size to the FLAG antibody in the FLAG-tagged mutants. Furthermore, our antibody can detect and precipitate a protein of similar size from CFT073 wild-type cell lysates (Fig. 9).

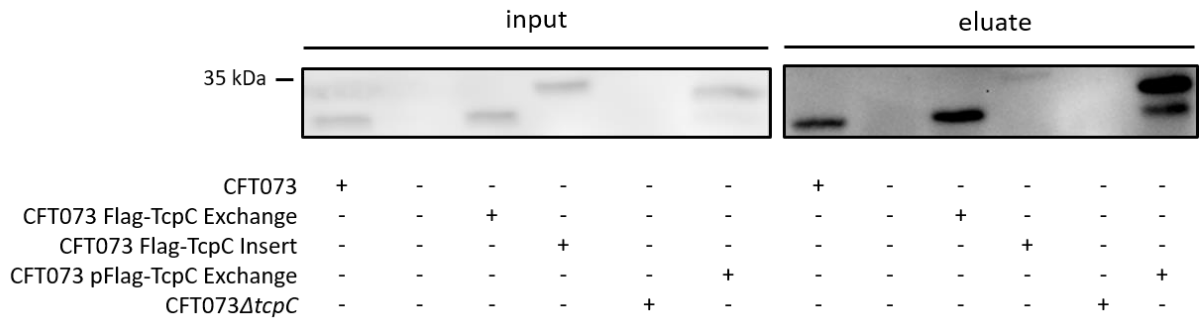

Figure 9 FLAG-tagged TcpC can be precipitated via TcpC antibody.

20 ml LB medium was inoculated with an overnight culture of CFT073 strains in a 1:100 dilution. The cultures were then incubated at 37°C, 200 rpm for 3 hours, after which the bacteria were pelleted by centrifugation. The cells were lysed using lysozyme, SDS lysis buffer, and heat. CFT073 wildtype with FLAG-tagged TcpC encoded on pASK-IBA5plus served as a positive control, and CFT073*ΔtcpC* served as a negative control. The input fraction represents proteins in solution before immunoprecipitation, and the eluate represents proteins precipitated from the input with our TcpC antibody. The samples were run on a 12% SDS gel and visualized with our TcpC primary antibody.

I initially wanted to use these mutants in infections of monocytes and macrophages to be able to detect TcpC through the FLAG-tag in case our TcpC antibody was not working properly in an endogenous context. In order to do that, I had to show that the insertion of the FLAG-tag preserves the function of TcpC in infections. One infection of THP-1 monocytes with the FLAG-tagged CFT073 mutants, indeed, showed that the mutants seem to have the same stimulatory capabilities as CFT073 wild-type (Fig 10). I chose the site of the FLAG-tag insertion where I thought the chance of it interfering with the function of TcpC would be the least. An AlphaFold model of TcpC showed that a less-structured region lies in front of the TIR domain compared to the rest of the protein. I thought this region was a linker sequence between the C-terminal half, which contains the transmembrane region, and the N-terminal part, which contains the TIR domain. Additionally, the change in size through the addition of the FLAG-tag and the FRT site does not seem to influence the function of TcpC as the stimulatory capacity between CFT073 wild-type and the two FLAG-tag mutants did not differ. However, I only performed this infection experiment once because the preceding analysis of our TcpC antibody showed excellent recognition of TcpC. That is why the need to use the FLAG-tagged mutants became redundant.

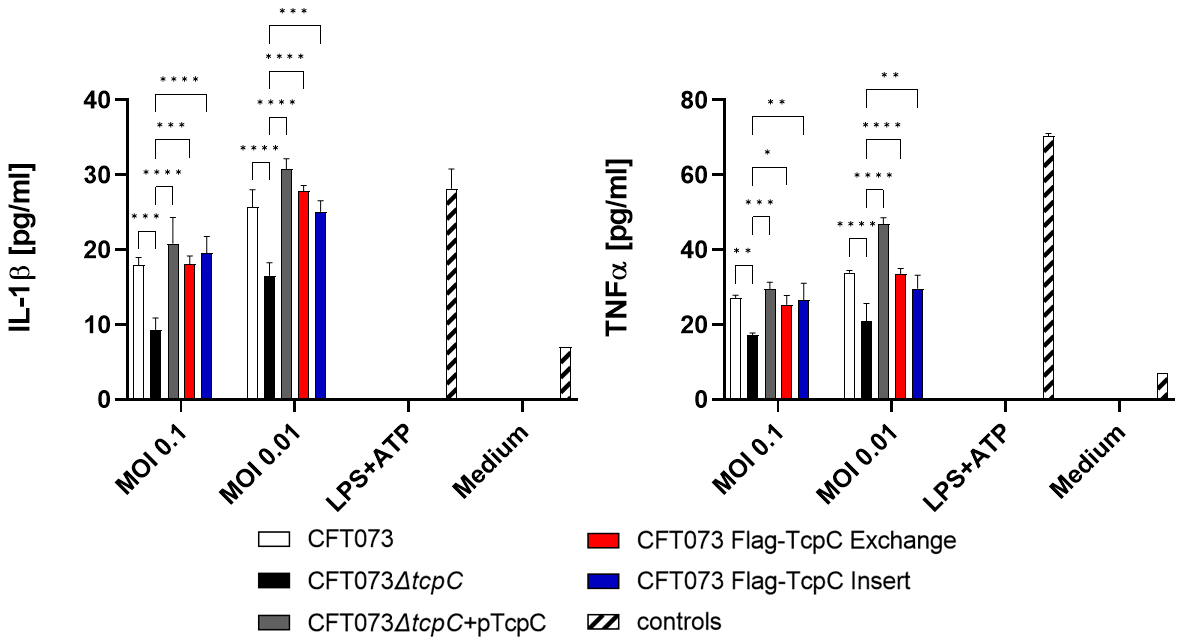

Figure 10 TcpC of FLAG-tag mutants retains function.

THP-1 monocytes were infected with the indicated MOIs for 5 hours, after which culture supernatants were collected and cytokine release of the cells was measured with ELISA. Stimulation with 100 ng/ml LPS with an addition of 5 µM ATP, 4 hours post-infection, served as a positive control, and treatment with infection medium served as a negative control. Statistical analysis was done by 2-way ANOVA and post-hoc Tukey test using GraphPad Prism. Data is shown as mean and SD of one experiment performed in triplicate.

3.5 Overexpression and detection of TcpC in culture supernatants

I can see that, during an infection of monocytes and bladder epithelial cells, TcpC is able to stimulate the release of proinflammatory cytokines. However, the mechanism by which TcpC is able to modulate the immune response of these cells is not clear. I asked the question whether TcpC is able to influence the immune response in a dose-dependent manner. This experiment cannot be done by increasing the MOI of bacteria used in an infection because I observed that infecting THP-1 monocytes or PBMCs with an MOI of 1 results in very low or not measurable release of TNFα, presumably because all cells are killed. As an alternative, I cloned TcpC into the vector pASK-IBA5plus, an anhydrotetracycline-inducible vector, and transformed it into CFT073*ΔtcpC*. I then planned to infect THP-1 monocytes with this strain and to induce the expression of TcpC in increasing strengths by incrementally increasing the concentration of anhydrotetracycline.

Fig. 11 A shows that the incremental increase in anhydrotetracycline increases the expression of TcpC from pASK-IBA5plus in the cytosol in a dose-dependent manner. The experiment also revealed that the repressor system of the vector does not completely suppress expression of TcpC, resulting in a basal expression of the protein even without induction. The expression level is higher compared to endogenous expression of TcpC, most likely because the pASK-IBA vectors are high-copy vectors, leading to multiple copies of the plasmid per bacterium. I can also see a band at around 15 kDa besides the full-length TcpC. This corresponds to roughly half the size of TcpC. The TcpC antibody binds to a motif at the C-terminus of TcpC, meaning that the fragment at 15 kDa is most likely the TcpC TIR domain. This indicates that TcpC might be processed by CFT073, and it can have more than one isoform.

I also show that the induction of the vector leads to growth inhibition in a dose-dependent manner. The stronger the vector is induced, the more the growth of the bacteria is inhibited (Fig. 11 B).

The infection of THP-1 monocytes with CFT073*ΔtcpC*+pASK-TcpC and subsequent induction of the vector to overexpress TcpC during the infection were performed by my colleague Hannah Griffith. She showed that increasing the induction of TcpC overexpression during the infection leads to an increase in the release of IL-1β and TNFα in a dose-dependent manner. Since the induction of TcpC expression dose-dependently inhibits the growth of the bacterium, it is likely that the stimulatory capacity of CFT073 decreases with higher concentrations of Atc. It seems that increasing the amount of TcpC during the infection leads to an increased proinflammatory response even though the stimulus by the bacteria becomes weaker due to growth retardation. I then looked for ways to induce the endogenous expression of TcpC to be independent of the growth retardation caused by the vector. Additionally, I looked at ways to generate samples with TcpC, separate from the bacteria, so I can treat monocytes with TcpC during LPS plus ATP stimulation to be independent of the cytotoxic effects caused by the bacteria.

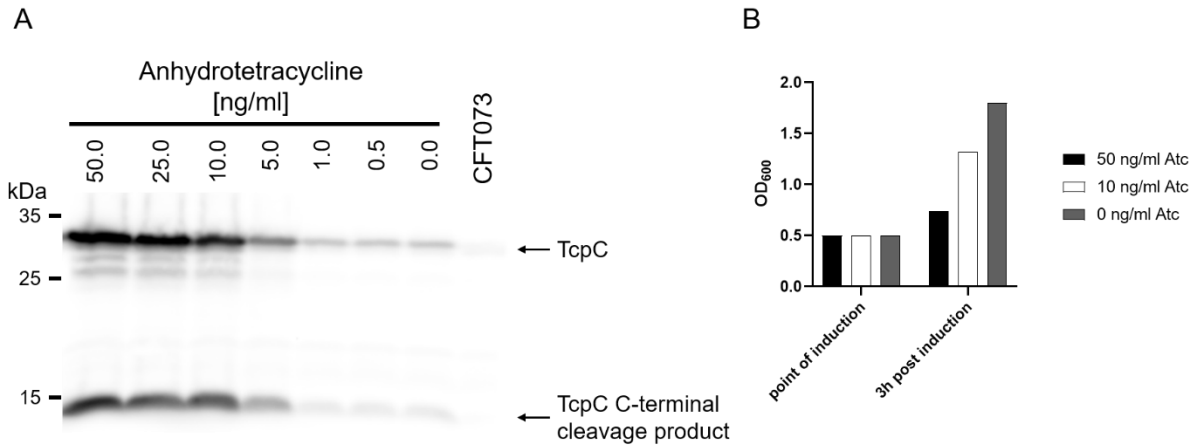

Figure 11 Dose-dependent induction of TcpC in pASK-IBA5plus.

140 ml LB medium was inoculated with CFT073*ΔtcpC*+pASK-TcpC, and 20 ml LB medium was inoculated with CFT073 wild-type overnight culture in a dilution of 1:100. The cultures were incubated at 37°C, 200 rpm until the plasmid strain reached an OD_{600} of 0.5. The 140 ml were then split into 7x 20 ml cultures and induced with the indicated concentrations of anhydrotetracycline. The cultures were incubated for one more hour, after which the bacteria were pelleted by centrifugation and lysed. 40 µg total protein was run on a 12% SDS gel and detected with our TcpC primary antibody (A). 60 ml LB medium was inoculated with CFT073*ΔtcpC*+pASK-TcpC overnight culture in a dilution 1:100. The cultures were incubated at 37°C, 200 rpm until an OD_{600} of 0.5 was reached. The culture was split into 3x 20 ml and induced with the indicated concentrations of anhydrotetracycline. After 3 hours of incubation, the OD_{600} was measured to evaluate the impact of induction of TcpC expression on bacterial growth (B).

Since colleagues before me were unable to overexpress and purify full-length TcpC, I decided to try a different strategy. I wanted to work with full-length TcpC because I believe truncating the protein might influence its function. I decided to express TcpC into culture supernatants utilizing the basal expression of the pASK-IBA5plus vector. Before treating cells with the supernatants, I had to confirm that TcpC was secreted into the culture supernatants. I first incubated CFT073, CF073*ΔtcpC*, CF073*ΔtcpC*+pASK-TcpC, and CF073*ΔtcpC*+pASK-TcpCΔTIR in 60 ml cultures of RPMI containing 3% FCS. Fig. 12 A shows that TcpC is expressed from the vector in the cytoplasm. CF073*ΔtcpC*+pASK-TcpCΔTIR does not produce a protein detectable by our TcpC antibody because it binds to a sequence at the C-terminus, which is missing after deleting the TIR domain. Although I could detect cytoplasmic TcpC from the culture in RPMI + 3% FCS, I was not able to perform a western blot from the culture supernatant. To detect TcpC in the culture supernatant, I have to concentrate it 150-fold, and the subsequent concentration of FCS proteins interferes with the SDS gel. Alternatively, I produced culture supernatants in a 60 ml culture with only RPMI. Here,

I could also detect cytoplasmic TcpC (Fig. 12 A), and in the samples of CF073*ΔtcpC*+pASK-TcpC, I see the C-terminal fragments seen in Fig. 11 again. However, the increase of this fragment in the bacteria cultured in RPMI containing FCS was not reproducible. I was able to analyse the 150-fold concentrated culture supernatants obtained from growing CF073*ΔtcpC*+pASK-TcpC in only RPMI on a western blot. Fig. 12 B shows that TcpC is secreted into the culture supernatant in these conditions. Notably, I had to concentrate the culture supernatant of a 60 ml culture 150-fold to detect a faint band of TcpC from CFT073 wild-type. That leads me to the assumption that TcpC might not be present in large quantities during infections. From this, I also assume that TcpC is secreted in the cultures of RPMI in the presence of 3% FCS, however, I am not able to prove that at the moment.

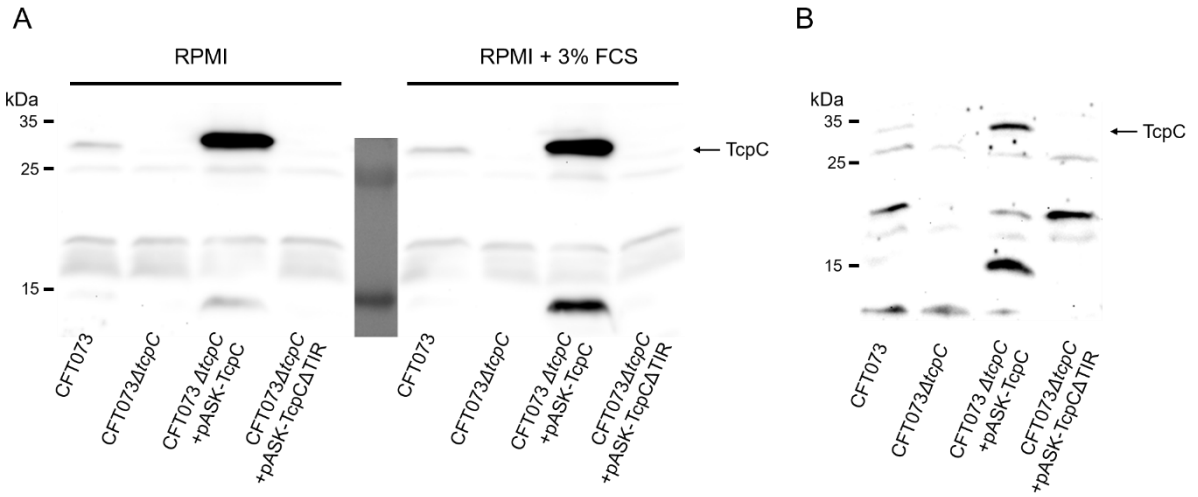

Figure 12 TcpC is secreted into the culture supernatant.

60 ml cultures were inoculated with overnight cultures and grown to an OD_{600} of 0.5 in LB. The bacteria were then washed three times with RPMI and transferred to either 60 ml RPMI or RPMI + 3% FCS and incubated for 3 hours, after which bacteria and culture supernatants were separated. Samples were run on a 12% SDS gel, and TcpC was detected with a western blot and our TcpC antibody. The western blots represent 1 of 2 independent experiments.

3.6 TcpC in culture supernatants suppresses response to LPS plus ATP in monocytes

The treatment of THP-1 monocytes with bacterial culture supernatants containing TcpC led to surprising results. While during infection with the CFT073 strains, the presence of TcpC causes a stimulation of proinflammatory cytokine release compared

to the infection with the TcpC knockout mutant, TcpC in the culture supernatants seems to suppress the release of the proinflammatory cytokines IL-1β and TNFα.

THP-1 cells were treated with culture supernatants in which expression of TcpC from pASK-IBA5plus was not induced and relied on the leaky basal expression of the vector, culture supernatants in which TcpC expression was induced with 10 and 50 ng/ml anhydrotetracycline, and a 50 ng/ml supernatant that was concentrated by a factor of two. Additionally, THP-1 cells were treated with a culture supernatant from the TcpC knockout mutant. The culture supernatant of the knockout mutant can stimulate THP-1 cells and induce a proinflammatory response, leading to the release of IL-1β and TNFα. This most likely occurs due to LPS and other PAMPs released by the bacteria during the cultivation period (Fig. 13 A). The culture supernatants containing TcpC this time showed reduced release of IL-1β and TNFα, suggesting that under these conditions, TcpC may potentially suppress the proinflammatory response (Fig. 13 A).

However, as I demonstrated earlier, induction of TcpC expression from pASK-IBA5plus inhibits bacterial growth, therefore, the reduced cytokine release could be due to fewer PAMPs in the culture supernatant. To address this issue, I added an additional 100 ng/ml LPS plus ATP to the THP-1 cells during treatment with the bacterial culture supernatants. The supernatants in which TcpC expression was induced still showed the ability to reduce the released IL-1β and TNFα compared to both, the cells treated with LPS plus ATP and the supernatant of the TcpC knockout mutant, and LPS plus ATP (Fig. 13 B). The most surprising finding was that the supernatant obtained from leaky vector expression, in many cases, inhibited cytokine release to such an extent that the ELISA could not measure their concentration. This suggests that TcpC has different effects depending on the presence or absence of CFT073, where it increases the release of proinflammatory cytokines when the bacteria are present and reduces cytokine release when they are absent.

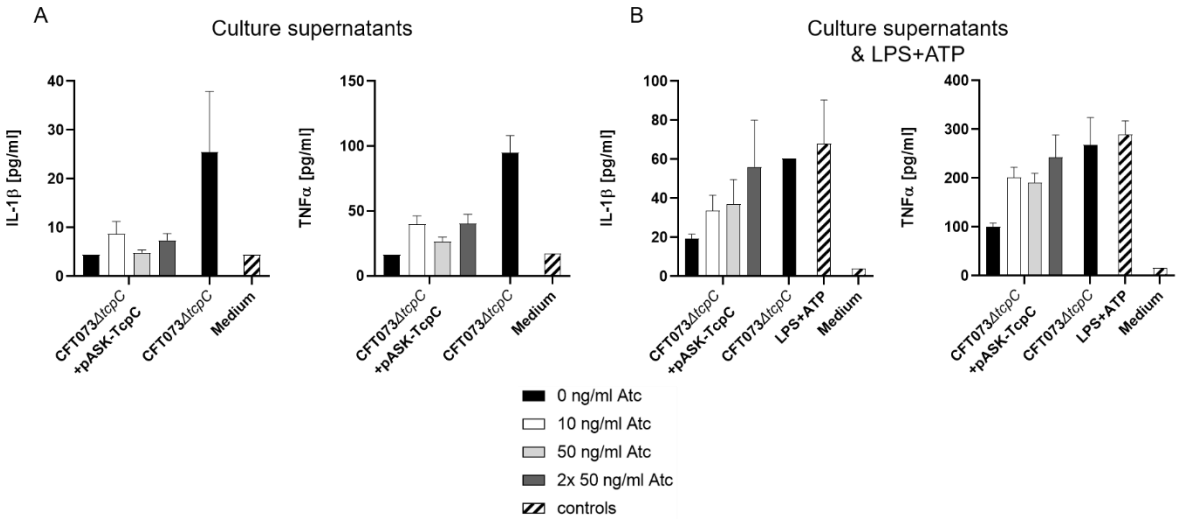

Figure 13 TcpC in culture supernatants suppresses the response to LPS.

THP-1 monocytes were treated with culture supernatants of CFT073*ΔtcpC* and CFT073*ΔtcpC*+pASK-TcpC and not stimulated with LPS+ATP (A) or stimulated with LPS+ATP (B). CFT073*ΔtcpC*+pASK-TcpC was induced with indicated concentrations of anhydrotetracycline (Atc) during the production of the culture supernatants. THP-1 cells were treated for 3 hours, after which supernatants were collected and released cytokines were measured with ELISA. Stimulation with 100 ng/ml LPS with an addition of 5 µM ATP, 2 hours post-stimulation, served as a positive control, and treatment with infection medium served as a negative control. (A) represents the mean and SD of one experiment, and (B) represents the mean and SEM of 2 independent experiments.

Just 0.5 ml of the culture supernatant from a 20 ml culture is able to suppress a response to 100 ng/ml LPS. I was therefore wondering how strong the suppressive effect of TcpC in the culture supernatants might be. I stimulated THP-1 monocytes with LPS concentrations ranging from 10 ng/ml to 1 µg/ml for 3 hours, and additionally treated them with TcpC-containing culture supernatants or only LPS plus ATP. The group only stimulated with LPS plus ATP shows that the THP-1 monocytes release IL-1β (Fig. 14 A) and TNFα (Fig 14 B) in a dose-dependent manner. The cytokine release increases with the strength of the LPS stimulation. When adding the TcpC-containing culture supernatants to the LPS-stimulated cells, the cytokines released by the cells are barely measurable, showing a suppression of cytokine release over a wide range of LPS concentrations. This suggests a mechanism that is very efficient because I had to concentrate a 60 ml culture to a factor of 150 to detect TcpC on a western blot.

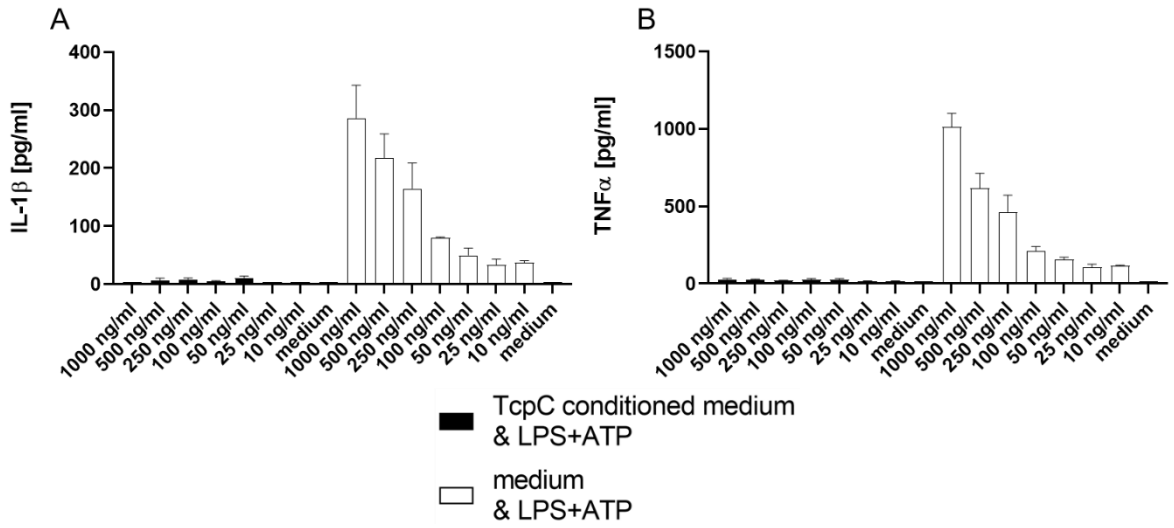

Figure 14 TcpC in culture supernatants suppresses an LPS response up to 1 µg/ml.

THP-1 monocytes were treated with culture supernatants of CFT073*ΔtcpC*+pASK-TcpC or only infection medium and stimulated with the indicated concentrations of LPS. CFT073*ΔtcpC*+pASK-TcpC was not induced during the production of the culture supernatants. THP-1 cells were treated with the indicated concentrations of LPS for 3 hours with an addition of 5 µM ATP, 2 hours post-stimulation, after which supernatants were collected and released cytokines were measured with ELISA. Stimulation with 100 ng/ml LPS with an addition of 5 µM ATP, 2 hours post-stimulation, served as a positive control, and treatment with infection medium served as a negative control. The graphs represent the mean and SD of one experiment.

I then wondered whether stimulation of THP-1 monocytes by LPS could be restored by deleting the TIR domain from TcpC or by diluting the culture supernatants. Dilution of the TcpC-containing culture supernatants increases the release of IL-1β and TNFα upon LPS stimulation. At a dilution of 1:100, the IL-1β (Fig. 15 A) release is almost restored to the level of the LPS stimulation, and TNFα (Fig. 15 B) is completely restored to the level of the LPS stimulation. The deletion of the TIR domain and only expressing the first 183 amino acids into the culture supernatant restores the response to an LPS stimulation as well, demonstrating that it is the TIR domain of TcpC that suppresses it.

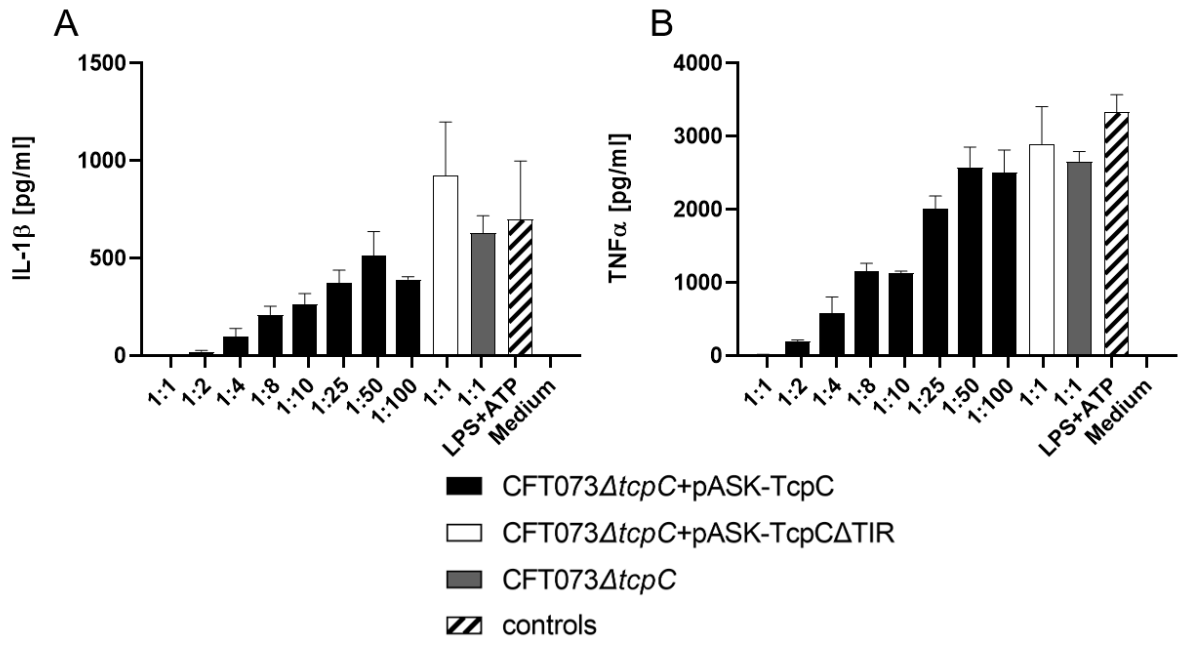

Figure 15 Suppression of LPS response is TcpC dose-dependent and depends on the TIR domain.

THP-1 monocytes were treated with culture supernatants of CFT073*ΔtcpC*, CFT073*ΔtcpC*+pASK-TcpC or CFT073*ΔtcpC*+pASK-TcpCΔTIR. CFT073*ΔtcpC*+pASK-TcpC and CFT073*ΔtcpC*+pASK-TcpCΔTIR were not induced during the production of the culture supernatants. THP-1 cells were stimulated with 100 ng/ml LPS for 3 hours, after which supernatants were collected and released cytokines were measured with ELISA. Stimulation with 100 ng/ml LPS with an addition of 5 µM ATP, 2 hours post-stimulation, served as a positive control, and treatment with infection medium served as a negative control. The graphs represent the mean and SD of one experiment.

I was not able to detect TcpC from culture supernatants that were produced in RPMI containing 3% FCS because the accumulation of proteins from the FCS during the concentration of the culture supernatants interfered with the SDS gels. That is why I also had TcpC-containing culture supernatants produced in RPMI without FCS. Treating LPS-stimulated THP-1 monocytes with these culture supernatants revealed that TcpC, which was produced by CFT073*ΔtcpC*+pASK-TcpC in RPMI without FCS, is not able to suppress the response to LPS (Fig. 16 A). The influence of FCS on the function of TcpC is still unknown. The interesting part is that during the treatment of the THP-1 monocytes, both groups, the one treated with TcpC-containing supernatants produced in RPMI (Fig. 16 A) and the one treated with TcpC-containing supernatants produced in RPMI containing 3% FCS (Fig. 16 B), were incubated in RPMI containing 3% FCS together with the THP-1 monocytes. Therefore, I conclude that the difference in effect must come from the presence or absence of FCS during TcpC expression in CFT073.

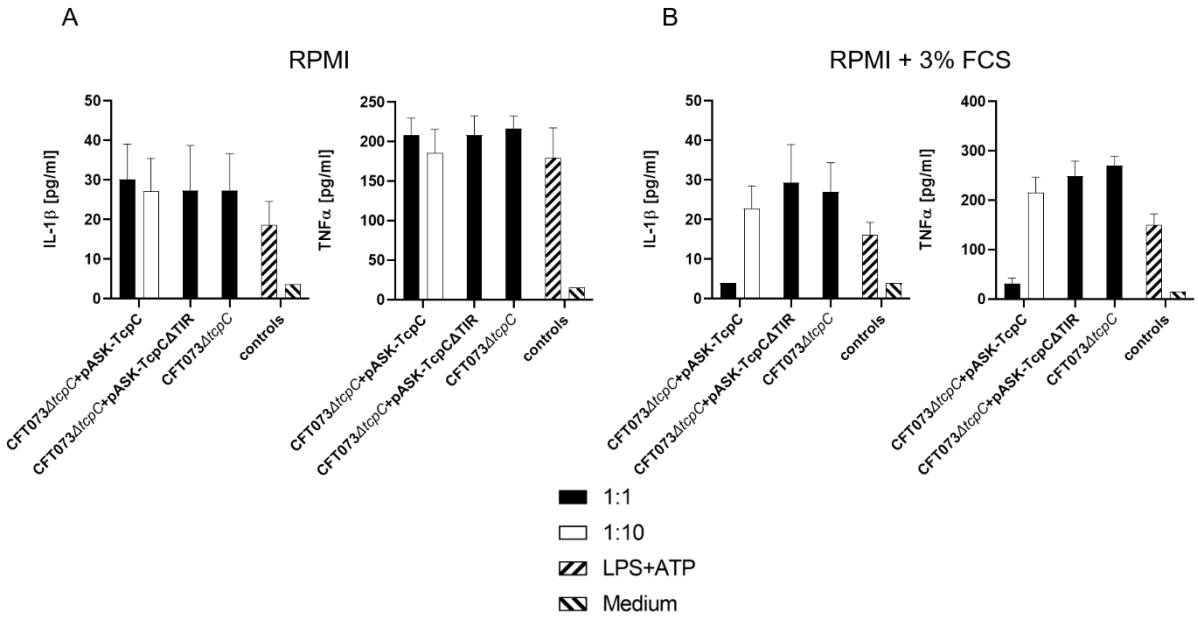

Figure 16 Suppression of LPS response depends on FCS during the production of supernatants.

THP-1 monocytes were treated with culture supernatants of CFT073*ΔtcpC*, CFT073*ΔtcpC*+pASK-TcpC or CFT073*ΔtcpC*+pASK-TcpCΔTIR produced in RPMI that did not or did contain 3% FCS during their production. CFT073*ΔtcpC*+pASK-TcpC and CFT073*ΔtcpC*+pASK-TcpCΔTIR were not induced during the production of the culture supernatants. THP-1 cells were stimulated with 100 ng/ml LPS for 3 hours, with an addition of 5 µM ATP, 2 hours post-stimulation, after which supernatants were collected and released cytokines were measured with ELISA. Stimulation with 100 ng/ml LPS with an addition of 5 µM ATP, 2 hours post-stimulation, served as a positive control, and treatment with infection medium served as a negative control. The graphs represent the mean and SEM of two independent experiments.

3.6 Potassium increases TcpC expression

Hemberger, et al., 2022 demonstrated that potassium induces the TcpC promoter. I wanted to further investigate whether the promoter induction results in a higher TcpC expression, as this would be a possibility to manipulate the amount of endogenous TcpC that is produced during an infection. I prepared overnight cultures in M9 minimal medium containing no potassium and split the overnight culture into one culture in M9 minimal medium without potassium and one culture containing an additional 200 mM KCl. The bacteria generally grew very slowly in the minimal medium, which is why I decided to perform an immunoprecipitation of TcpC. Western blots of the lysed cell fractions revealed that potassium seems to be able to increase TcpC protein levels, as faint bands can be seen in the samples of CFT073 wild-type treated with potassium (Fig. 17 A). Band density analysis of the precipitated TcpC normalized to GAPDH

confirmed that potassium increased production of TcpC by approximately two-fold (Fig. 17 B).

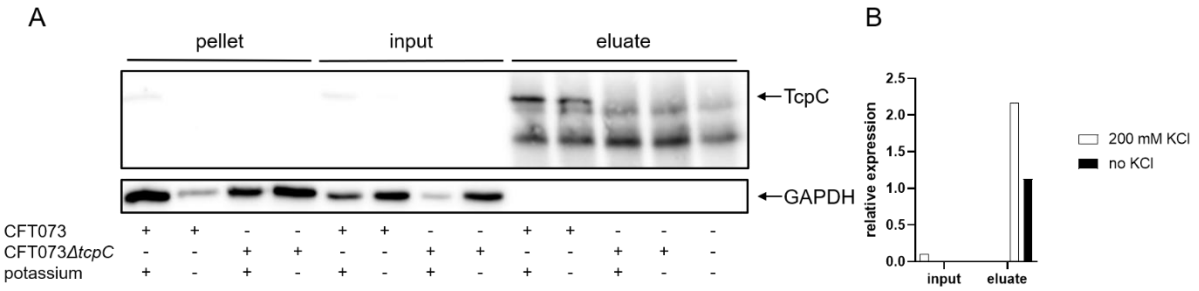

Figure 17 Endogenous TcpC expression is inducible with Potassium.

CFT073 and CFT073*ΔtcpC* were cultured in M9 minimal medium that did not contain any potassium overnight. They were transferred to M9 minimal medium with or without 200 mM KCl and cultured for 4 hours, after which bacterial cells were collected, lysed, and TcpC was precipitated. The TcpC production was then analysed with western blot (A). GAPDH was used as a loading control and standard for band density measurements. Band density measurements were performed using FIJI (B).

3.7 TcpC does not affect expression of myddosome proteins

I think of two possibilities for how TcpC modulates the innate immune response: its interaction with myddosome and the NLRP3 inflammasome. TcpC was shown to bind to TLR4 and MyD88. To address these questions, I started analyzing the expression of the myddosome proteins after infection and LPS stimulation.

The myddosome forms shortly after TLR4 activation, and I expected the proteins to be detectable after 30 – 60 minutes. I also expected that the myddosome forming after the initial LPS stimulation would dissociate after some time to avoid sustained signal transduction. That is why I chose two time points for the detection after LPS stimulation: 1 hour post-stimulation and 4 hours post-stimulation. The western blot of total cytosolic protein (Fig. 18 A) shows that the three proteins comprising the myddosome - MyD88, IRAK2, and IRAK4 - are present in THP-1 cells and are detectable. One hour of LPS stimulation seems to increase the expression of the myddosome proteins slightly. After four hours, this difference is not visible anymore, the amount of IRAK2 in the cells even seems to be reduced. These results need to be confirmed by more repititions

Additionally, I infected T24/83 cells with CFT073, the TcpC knockout mutant, and the recomplemented strain. I decided to use T24/83 cells because they seem more robust and better at dealing with infections than the monocytes. I assumed that the cells would not respond identically to the infection with the bacteria and to the LPS stimulation,

which is why I started with a 4 hour infection. Fig. 18 B shows that an infection or LPS stimulation indeed does not elicit the same response of the T24/83 as there seems to be more IRAK2 and less IRAK4 and MyD88 produced during the infection with CFT073. There is also no difference in protein expression depending on TcpC. However, these findings are not conclusive because, for comparability, a loading control and more repetitions would be needed.

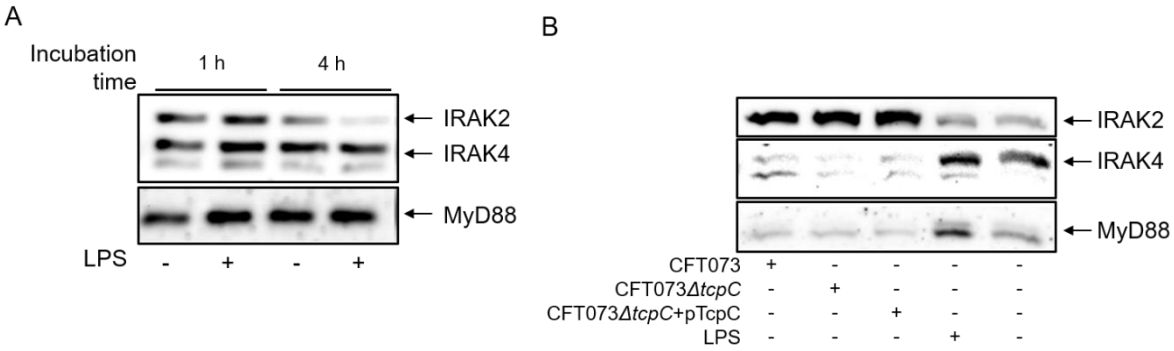

Figure 18 TcpC does not affect expression of myddosome proteins.

THP-1 monocytes were treated with 100 ng/ml LPS or left unstimulated for 1 and 4 hours, after which the cells were collected and total cytosolic proteins were extracted (A). T24/83 cells were infected with CFT073 wild-type, CFT073*ΔtcpC,* or CFT*ΔtcpC*+pTcpC for 4 hours, after which the cells were collected and total cytosolic proteins were extracted. Stimulation with 100 ng/ml LPS served as a positive control, and treatment with the infection medium served as a negative control (B). The samples were run on a 12% SDS gel and visualized with he indicated primary antibody on the right.

4 Discussion

In this project, I show that the virulence factor TcpC of uropathogenic *E. coli* CFT073 can both induce and suppress a proinflammatory immune response, as reflected in increased or decreased release of the proinflammatory cytokines IL-1β, TNFα, and IL-6. Thereby, TcpC appears to modulate innate immune checkpoints in two distinct ways, depending on the presence or absence of bacteria. While infection with TcpC-producing CFT703 increases the release of proinflammatory cytokines from monocytes and bladder epithelial cells, treatment of monocytes with TcpC protein from culture supernatants suppresses the immune response upon LPS plus ATP stimulation.

4.1 TcpC as a positive modulator of innate immune checkpoints

Here, I show that TcpC stimulates the release of the proinflammatory cytokines IL-1β, TNFα, and IL-6 during an infection of PBMC (Fig. 2), peripheral blood monocytes (Fig. 3) and the bladder cell line T24/83 (Fig. 5) compared to the TcpC-deficient mutant CFT073*ΔtcpC*. The recomplementation of CFT073*ΔtcpC* with the vector pYCAC184 encoding TcpC under control of its endogenous promotor restores the stimulation of cytokine release. Previous studies largely reported that TcpC suppresses the innate immune response, which at first contradicts my data of a stimulation of a proinflammatory response (Cirl, et al., 2008; Fang, et al., 2021; Waldhuber, et al., 2016). However, even the data from these studies are not completely one-sided. Yadav et al. reported that C57BL/6 mice infected with CFT073 wild-type had elevated MIP-2 during the whole 6 days of infection compared to mice infected with TcpC-deficient CFT073*ΔtcpC*. MIP-2 is a homologue of human IL-8 in mice (Mittal, et al., 2004) and is responsible for the recruitment of neutrophils during UTIs in mice (Hang, et al., 1999). The elevated PMN numbers in urine and the formation of kidney abscesses in the mice infected with CFT073 indicated that the increased MIP-2 indeed led to higher neutrophil migration to the infection, since neutrophils can cause abscess formation by IL-1β production (Cho, et al., 2012). This is all indicative of a stimulation of the innate immune response and would correspond with my findings that TcpC can stimulate proinflammatory cytokine release during infection.

The local induction of the release of specific proinflammatory cytokines might even be beneficial for CFT073, as Porat et al. reported that concentrations of 10 ng/ml IL-1β could stimulate the growth of virulent *E. coli* (Porat, et al., 1991, Porat, et al., 1992), and recombinant mouse TNFα was also able to stimulate the growth of *E.* coli (Lee, et al., 2003). This could indicate that CFT073 prefers a milieu containing specific proinflammatory cytokines, as they promote its proliferation.

I believe one of the primary targets of TcpC is the myddosome due to its ability to directly interact with the TIR domains of TLR4 and MyD88 (Snyder, et al., 2013). However, infections of MyD88-deficient T24/83 cells show that TcpC still stimulates TNFα and IL-6 release in the absence of the adapter protein. This suggests that TcpC may interact with the MyD88-independent pathway of TLR4. The TRIF pathway of TLR4 is the so-called non-canonical pathway. It is activated by endosomal TLR4 and leads to NF-κB activation and the production of type I interferon (Ullah, et al., 2016). Because the infection of TLR4-deficient T24/83 cells produced no TcpC-dependent phenotype anymore, the target for TcpC has to be related to the activation of this receptor and innate immune checkpoint. This could indicate TRIF as an additional target for TcpC.

The increased IL-1β release caused by TcpC could also benefit CFT073 due to the nature of how IL-1β is mainly released. Since IL-1β does not have a signal peptide for canonical secretion, it is secreted by the activation of gasdermin D by the NLRP3 inflammasome. The activation of the pore-forming protein gasdermin D leads to the programmed cell death called pyroptosis, which most likely leads to the efflux of potassium due to the osmotic gradient. I show that TcpC expression is stimulated by potassium (Fig. 17), which would create a positive feedback loop that causes increased TcpC expression through activation of the NLRP3 inflammasome. During the endogenous overexpression of TcpC using potassium, I also noticed that CFT073 grew better in the minimal medium containing potassium (data not shown), which could indicate that the release of intracellular potassium through pyroptosis of the immune cells can have a positive effect on the growth of CFT073.

4.2 TcpC as a negative modulator of innate immune checkpoints

TcpC in culture supernatants is very potent at suppressing the response of monocytes to LPS plus ATP stimulation. Snyder, et al., 2013 resolved the crystal structure of the MyD88 TIR domain and demonstrated that the TcpC TIR directly interacts with MyD88 and TLR4 with its BB and DD loops. A BB loop-derived peptide was able to inhibit responses to LPS stimulation, and a DD loop-derived peptide inhibited multiple TLR ligands. They propose that the interaction of the TcpC TIR domain with TLR4 and MyD88 might impair their ability to form active complexes via TIR-TIR interactions. This assumption implies that TcpC would competitively bind the TLR4 and MyD88 TIR domains. The detection of TcpC in culture supernatants revealed that it is secreted at very low levels by CFT073, as a 150-fold concentration was required to detect endogenous TcpC by western blot (Fig. 12). That makes it less likely that TcpC inhibits cytokine release by competitively binding the myddosome proteins and more likely that TcpC inhibits the myddosome formation by a mechanism where one TcpC molecule can incapacitate multiple myddosomes. Fang, et al. propose that TcpC is an E3 ubiquitin ligase that promotes the degradation of MyD88. The potential E3 ubiquitin ligase function could not have been studied by Snyder et al. because they exclusively used the TcpC TIR domain, while Fang et al. propose the active center for the E3 ubiquitin ligase is located at the N-terminus, whereas the TIR domain makes up the C-terminal half of the protein. The ubiquitin ligase function would fit better with my observations that TcpC can inhibit the release of proinflammatory cytokines upon LPS stimulation at low levels. One TcpC molecule could neutralize multiple MyD88 molecules and thereby prevent the adapter protein from being recruited to TLR4. Fang, et al. show that kidney macrophages from mice infected with CFT073 have significantly less MyD88 compared to kidney macrophages from mice infected with CFT073*ΔtcpC*. Western blots of THP-1 cells treated with the TcpC-containing culture supernatants and LPS plus ATP should also show lower levels of MyD88 compared to THP-1 cells treated with supernatants from CFT073*ΔtcpC* and LPS plus ATP. Additionally, the deletion of the TcpC TIR domain leads to the loss of the inhibitory capabilities of the TcpC-containing culture supernatants, demonstrating that the TcpC TIR domain is still a key factor for the inhibition (Fig. 15 & 16).

Another surprising find was that the presence of FCS during TcpC expression seems to affect its function, as TcpC expressed in the presence of FCS is able to suppress the response of monocytes to LPS, whereas TcpC expressed in the absence of FCS

does not have any effect on the release of IL-1β and TNFα upon LPS stimulation (Fig 16). FCS contains proteins that are important for TLR signaling like LPS-binding protein (Bochsler, et al., 1996). It was shown that LPS-binding protein is important for the proinflammatory innate immune response in mice when challenged with *E. coli* (Knapp, et al., 2003). Possibly, during the expression of TcpC in the presence of FCS, it forms complexes with LPS-binding protein that prevent TLR4 signaling in the treated THP-1 monocytes. Another possible explanation could be that during the concentration of the supernatants with the 10 kDa mwco centrifugal filter, an important co-factor, smaller than 10 kDa, that is bound in the presence of FCS, is lost during the concentration step in the supernatant in which TcpC was expressed without FCS. To get further insights into the role of FCS modulating TcpC function further research is needed.

4.3 TcpC does not promote invasion of bladder cells

A common hallmark of UPECs is the invasion of bladder epithelial cells (Kim, et al., 2018). It is also reported that UPECs evade the early innate immune response by forming so-called intracellular bacterial communities (IBCs) in bladder epithelial cells, and this might be one factor in recurring UTI, where bacteria break out after the first immune response and cause a new inflammation (Anderson, et al., 2004; Kwak, et al., 2024). My data show that TcpC does not promote the invasion of CFT073 into the bladder cell line T24/83, which means it is not involved in the formation of IBCs (Fig.7). One notable observation, independent of TcpC, was that MyD88-deficient T24/83 cells take up considerably, but not statistically significantly, less *E. coli*. It was shown that in macrophages, MyD88 supports the uptake and phagocytosis of *B. burgdorferi* ((Shin, et al., 2009; Benjamin, et al., 2021), but whether this data is transferable to bladder cells and *E. coli* is uncertain.

4.4 Overexpression of TcpC harms CFT073 but promotes a proinflammatory response

That TcpC is able to stimulate the release of proinflammatory cytokines from eukaryotic cells is a new finding, and I wanted to further explore this observation by infecting THP-1 monocytes with CFT073*ΔtcpC* recomplemented with the anhydrotetracycline-

inducible vector pASK-IBA5plus encoding TcpC. The expression of TcpC from pASK-IBA5plus is incrementally inducible (Fig. 11 A), and I transferred that to infection experiments where I could control the amount of TcpC during the infection. Upon infection of THP-1 monocytes, I observed a dose-dependent increase in IL-1β and TNFα release, but conversely, I observed a dose-dependent decrease in bacterial growth. This growth inhibition is infection-independent, as I also observe reduced growth when inducing overexpression in LB medium (Fig. 11 B). I believe this might happen because TcpC can hydrolyse and deplete NAD^+, disrupting its own energy household. Several TIR domains from bacterial proteins have been shown to have NAD^+ hydrolase activity, including the TcpC TIR domain (Essuman, et al., 2018). This could also explain why I observe such low TcpC expression. CFT073 simply cannot express the protein abundantly into the cytoplasm without harming itself.

While a stronger induction of TcpC overexpression leads to more TcpC being produced by the bacteria, the bacterial load is decreased due to growth inhibition. That also means we have to consider two factors in these infections. The stimulatory capacity of TcpC versus the stimulatory capacity of the bacterial PAMPs. This again shows the stimulatory capacities of TcpC during an infection, because even though the stimulatory potential of CFT073 decreases due to the growth inhibition, the proinflammatory response of the THP-1 cells increases with increased TcpC induction.

4.5 Mechanisms by which TcpC modulates the innate immune response

That TcpC can both stimulate and inhibit the innate immune response was shown by Yadav, et al., and Fang, et al. as I described earlier. One important factor in which effect TcpC has could be the amount of TcpC. Lower amounts of TcpC could stimulate a proinflammatory response, as I described that it could benefit the growth of CFT073. It could help CFT073 to colonize the bladder and to further ascend the urinary tract to the kidneys. In the kidney TcpC might accumulate and higher amounts of TcpC then have an inhibitory effect. Accumulation of TcpC could, for example, lead to homodimerization, and the TcpC dimers have an E3 ubiquitin ligase function. This could also explain why I do not see the stimulatory effect when I dilute the culture supernatants during the treatment of LPS plus ATP stimulated THP-1 cells (Fig. 15). Another factor between the stimulatory and inhibitory effect of TcpC could be the direct contact between the bacteria and eukaryotic cells. Monocytes directly in contact with

CFT073 release more IL-1β and TNFα during the infection than monocytes in contact with the TcpC-deficient strain, while LPS plus ATP stimulation is inhibited in THP-1 cells treated with secreted TcpC in culture supernatants. CFT073 may produce other factors that support an increased proinflammatory response leading to immune cells becoming pyroptotic localized, and release cytokines and K^+ which may promote bacterial growth (Porat, et al., 1991; Lee, et al., 2003). Secreted TcpC further away from the bacteria may impair an immune response so that the increased proinflammatory response is contained localized around the bacteria. To get more insights into these two opposing phenotypes more research into TcpC has to be conducted.

Furthermore, the differentiation and polarization state seem to play a vital role in the effect of TcpC. While eliciting a stimulation of IL-1 β and TNFα release during infections of THP-1 and peripheral blood monocytes, the PMA differentiation of THP-1 cells into macrophages completely abrogates the TcpC-mediated stimulation and differentiation of peripheral blood monocytes into MDMs, considerably reduces the stimulatory effect of TcpC. Macrophages generally have more TLR4 and LPS-related receptors (Kim, et al., 2022; Jungi, et al., 1994). This could lead to a more robust response of macrophages as indicated by their stronger TNFα release, leaving less room for TcpC to modulate it. However, polarization of THP-1 M0 macrophages into M1-like macrophages restores the ability of TcpC to stimulate the release of TNFα and IL-6, but not IL-1β (Heine, et al., in revision). Contrary to that, polarization to an M2-like phenotype completely abrogated stimulation by bacteria. Interestingly, the cells still respond to LPS plus ATP stimulation by releasing IL-1β and TNFα.

The western blot of T24/83 cells infected with the CFT073 strains (Fig. 18 B) shows that TcpC has no effect on the expression of myddosome proteins, indicating that the stimulation of the proinflammatory response is not the result of an increased expression of myddosomes protein resulting in an increased abundance of myddosomes. I believe that TcpC can facilitate better formation of the myddosome complex by supporting the binding between MyD88 and TLR4. By facilitating more binding events of the myddosome or maintaining the activated myddosome for a longer time, TcpC causes an increased proinflammatory response following the activation of TLR4. Additionally, there is a difference between a pure LPS stimulation and the

stimulation by bacteria, signifying that LPS is suitable to elicit a TLR4 activation, but the stimulation by the bacteria during an infection is far more complex.

The effect of TcpC on myddosome and NLRP3 inflammasome formation can be investigated through co-IPs of the protein complexes in the presence and absence of TcpC. Precipitating these complexes after infection with the CFT703 strains could reveal that TcpC stimulates the release of proinflammatory cytokines by supporting the formation of more myddosomes or a larger inflammasome, or by maintaining these SMOCs for longer and promoting a continued proinflammatory response compared to the TcpC-deficient strain.

The co-IPs would also allow the investigation of the effect of TcpC in the culture supernatants on the myddosome and NLRP3 inflammasome, and whether TcpC acts differently on these SMOCs in the presence or absence of the bacteria.

4.6 TcpC in disease therapy

Urinary tract infections are among the most common infections worldwide and are commonly treated with antibiotics. Klein, et al., 2024, analyzed the antibiotic consumption from 2016 – 2023 in 67 countries, showing an increase of 16.3% and projecting a rise by 52.3% until 2030. The rise of antimicrobial resistance to antibiotics is categorized as one of the 10 threats to global health by the WHO and is an ever-growing concern. The Global Antimicrobial Resistance and Use Surveillance System (GLASS) of 2022 found that approximately 1 in 5 *E. coli*, the most common pathogen in UTIs, was resistant to first-line and second-line antibiotics (WHO, 2022).

This signifies the importance of alternative therapies to antibiotics. As 20 – 40% of E. coli in UTI are reported to harbor the *tcpC* gene, TcpC could be a novel approach to treat certain UTIs (Schubert, et al., 2010). More specifically, preventing the secretion of TcpC could be an effective approach to treating UTIs caused by CFT073 or other *E. coli* strains that produce TcpC for two reasons. Prevention of the secretion of TcpC will hinder *E. coli* from modulating the innate immune response to its advantage. Furthermore, I showed that during overexpression, accumulation of cytoplasmic TcpC inhibited the growth of CFT073 (Fig. 11 B). I attribute this growth inhibition to the NAD^+-consuming ability of the TcpC TIR domain, which interferes with the bacterial energy metabolism (Essuman, et al., 2018). By preventing the secretion and promoting the

accumulation of TcpC in the bacteria, one could impede the growth in the urinary tract. Cirl, et al. showed that the treatment of CFT073 with the efflux pump inhibitor phenylalanine-arginine-β-naphtylamide (PAβN) reduced the secreted TcpC. Treatment of RAW264.7 mouse macrophages with PAβN could also abrogate the effect of TcpC during an infection. This shows possible alternative or supplementary ways to antibiotics in treating UTIs.

The mechanism of secretion is currently unknown, and TcpC does not possess a signal peptide for secretion, and CFT073 is missing the genes for the type III secretion system (Welch, et al., 2002). Future projects would need to investigate the secretion of TcpC and whether there are compounds that are approved for treatment of humans and can improve the clearance of UTIs caused by CFT073.

Furthermore, the TcpC TIR domain was shown to improve the disease outcome in an autoimmune arthritis mouse model (Pasi, et al., 2016). More specifically, the TcpC TIR domain has been shown to downregulate the proinflammatory response via MyD88 in Th17 cells, which are a key contributor to arthritis disease progression. This suggests that the TcpC TIR domain may be able to treat other autoimmune diseases involving the activation of MyD88-dependent immune responses.

In conclusion, I can say that TcpC from uropathogenic *E. coli* positively and negatively modulates innate immune checkpoints of monocytes and bladder cells in order to increase its pathogenicity. More work is needed to fully understand the function of the protein and what role it plays during UTI caused by CFT073.

5 Literature

Abbas, A. K. & Andrew H. Lichtman, S. P., 2022. In: *Cellular and Molecular Immunology.* Philadelphia: Elsevier, pp. 1-11.

Abraham, S. N. & Miao, Y., 2015. The nature of immune responses to urinary tract infections. *Nat Rev Immunol,* 15(10), pp. 655-63.

Akira, S., Takeda, K. & Kaisho, T., 2001. Toll-like receptors: critical proteins linking innate and acquired immunity. *Nat Immunol,* 2(8), pp. 675-80.

Anderson, G. G., Dodson, K. W., Hooton, T. M. & Hultgren, S. J., 2004. Intracellular bacterial communities of uropathogenic Escherichia coli in urinary tract pathogenesis. *Trends Microbiol,* 12(9), pp. 424-30.

Benjamin, S. J. et al., 2021. Macrophage mediated recognition and clearance of Borrelia burgdorferi elicits MyD88-dependent and -independent phagosomal signals that contribute to phagocytosis and inflammation. *BMC Immunol,* 22(32).

Bernoux, M. et al., 2011. Structural and functional analysis of a plant resistance protein TIR domain reveals interfaces for self-association, signaling, and autoregulation. *Cell Host Microbe,* 9(3), pp. 200-211.

Bertani, B. & Ruiz, N., 2018. Function and Biogenesis of Lipopolysaccharides. *EcoSal Plus,* 8(1).

Bien, J., Sokolova, O. & Bozko, P., 2012. Role of Uropathogenic Escherichia coli Virulence Factors in Development of Urinary Tract Infection and Kidney Damage. *Int J Nephrol.*

Bochsler, P. N., Yang, Z., Murphy, C. L. & Carroll, R. C., 1996. Purification of lipopolysaccharide-binding protein from bovine serum. *Vet Immunol Immunopathol,* 51(3-4), pp. 303-14.

Caruso, R., Warner, N., Inohara, N. & Núñez, G., 2014. NOD1 and NOD2: signaling, host defense, and inflammatory disease. *Immunity,* 41(6), pp. 898-908.

CDC, 2025. *CDC Urinary Tract Infection.* [Online] Available at: https://www.cdc.gov/uti/about/index.html [Accessed 25 10 2025].

Cho, J. S. et al., 2012. Neutrophil-derived IL-1β is sufficient for abscess formation in immunity against Staphylococcus aureus in mice.. *PLoS Pathog,* 8(11).

Ciesielska, A., Matyjek, M. & Kwiatkowska, K., 2021. TLR4 and CD14 trafficking and its influence on LPS-induced pro-inflammatory signaling. *Cell Mol Life Sci,* 78(4), pp. 1233-1261.

Cirl, C. et al., 2008. Subversion of Toll-like receptor signaling by a unique family of bacterial Toll/interleukin-1 receptor domain-containing proteins. *Nat Med,* 14(4), pp. 399-406.

Crotty, S., 2015. A brief history of T cell help to B cells. *Nat Rev Immunol,* 15(3), pp. 185-9.

Domínguez-Medina, C. C. et al., 2020. Outer membrane protein size and LPS O-antigen define protective antibody targeting to the Salmonella surface. *Nat Commun,* 11(1), p. 851.

Doron, S. et al., 2018. Systematic discovery of antiphage defense systems in the microbial pangenome. *Science,* 359(6379).

ECDC, Stockholm. *European Centre for Disease Prevention and Control. Point prevalence survey of healthcareassociated infections and antimicrobial use in European long-term care facilities,* 2025: s.n.

El-Zayat, S. R., Sibaii, H. & Mannaa, F. A., 2019. Toll-like receptors activation, signaling, and targeting: an overview. *Bull Natl Res Cent,* 43(187).

Essuman, K. et al., 2018. TIR Domain Proteins Are an Ancient Family of NAD+-Consuming Enzymes. *Curr Biol,* 28(3), pp. 421-430.

Fang, J.-Q.et al., 2021. TcpC inhibits toll-like receptor signaling pathway by serving as an E3 ubiquitin ligase that promotes degradation of myeloid differentiation factor 88. *PLoS Pathog,* 17(3).

Fang, J. et al., 2022. TcpC Inhibits M1 but Promotes M2 Macrophage Polarization via Regulation of the MAPK/NF-κB and Akt/STAT6 Pathways in Urinary Tract Infection. *Cells,* 11(17), p. 2674.

Farrell, K. et al., 2021. Treatment of uncomplicated UTI in males: a systematic review of the literature.. *BJGP Open,* 5(2).

Fischer, H. et al., 2007. Ceramide as a TLR4 agonist; a putative signalling intermediate between sphingolipid receptors for microbial ligands and TLR4. *Cell Microbiol,* 9(5), pp. 1239-51.

Gay, N. J., Gangloff, M. & O'Neill, L. A. J., 2011. What the Myddosome structure tells us about the initiation of innate immunity. *Trends Immunol,* 32(3), pp. 104-9.

Hang, L. et al., 1999. Macrophage inflammatory protein-2 is required for neutrophil passage across the epithelial barrier of the infected urinary tract.. *J Immunol,* 162(5), pp. 3037-44.

Hemberger, J. et al., 2022. The Promoter of the Immune-Modulating Gene TIR-Containing Protein C of the Uropathogenic Escherichia coli Strain CFT073 Reacts to the Pathogen's Environment. *Int J Mol Sci,* 23(3), p. 1148.

He, Y. et al., 2025. Epidemiological trends and predictions of urinary tract infections in the global burden of disease study 2021. *Scientific Reports,* 15(1), p. 4702.

Imler, J. L. & Hoffmann, J. A., 2002. Toll receptors in Drosophila: a family of molecules regulating development and immunity. *Curr Top Microbiol Immunol,* Volume 270, pp. 63-79.

Janeway Jr, C. A. & Medzhitov, R., 2002. Innate immune recognition. *Annu Rev Immunol,* Volume 20, pp. 197-216.

Jungi, T. W., Miserez, R. & M Brcic, H. P., 1994. Change in sensitivity to lipopolysaccharide during the differentiation of human monocytes to macrophages in vitro. *Experientia,* 50(2), pp. 110-4.

Kaper, J. B., Nataro, J. P. & Mobley, H. L., 2004. Pathogenic Escherichia coli. *Nat Rev Microbiol,* 2(2), pp. 123-40.

Kawai, T. et al., 2001. Lipopolysaccharide stimulates the MyD88-independent pathway and results in activation of IFN-regulatory factor 3 and the expression of a subset of lipopolysaccharide-inducible genes. *J Immunol,* 167(10), pp. 5887-94.

Kawasaki, T. & Kawai, T., 2014. Toll-like receptor signaling pathways. *Front Immunol,* Volume 5, p. 461.

Kelley, N., Jeltema, D., Duan, Y. & He, Y., 2019. The NLRP3 Inflammasome: An Overview of Mechanisms of Activation and Regulation. *Int J Mol Sci,* 20(13), p. 3328.

Kim, W.-J., Shea, A. E., Kim, J.-H. & Daaka, Y., 2018. Uropathogenic Escherichia coli invades bladder epithelial cells by activating kinase networks in host cells. *J Biol Chem,* 293(42), pp. 16518-16527.

Kim, Y. K., Hwang, J. H. & Lee, H. T., 2022. Differential susceptibility to lipopolysaccharide affects the activation of toll-like-receptor 4 signaling in THP-1 cells and PMA-differentiated THP-1 cells. *Innate Immunity,* 28(3-4), pp. 122-129.

Klein, E. et al., 2024. Global trends in antibiotic consumption during 2016–2023 and future projections through 2030. *Proc. Natl. Acad. Sci. U.S.A,* 121(49).

Knapp, S. et al., 2003. Lipopolysaccharide Binding Protein Is an Essential Component of the Innate Immune Response to Escherichia coli Peritonitis in Mice. *Infect Immun,* 71(12), pp. 6747-53.

Kuhn, H. W., Hreha, T. N. & Hunstad, D. A., 2023. Immune defenses in the urinary tract. *Trends Immunol,* 44(9), pp. 701-711.

Kwak, Y. et al., 2024. Critical Role of Intracellular Bacterial Communities in Uncomplicated Recurrent Urinary Cystitis: A Comprehensive Review of Detection Methods and Diagnostic Potential. *Int Neurourol J,* 28(1), pp. 4-10.

Lee, J.-H.et al., 2003. Modulation of bacterial growth by tumor necrosis factor-alpha in vitro and in vivo. *Am J Respir Crit Care Med,* 168(12), pp. 1462-70.

Li, S. et al., 2021. Cytosolic and nuclear recognition of virus and viral evasion. *Mol Biomed,* 2(1), p. 30.

Li, W. et al., 2016. Brucella TIR-like protein TcpB/Btp1 specifically targets the host adaptor protein MAL/TIRAP to promote infection. *Biochem Biophys Res Commun,* 477(3), pp. 509-14.

Luo, R., Yao, Y., Chen, Z. & Sun, X., 2025. An examination of the LPS-TLR4 immune response through the analysis of molecular structures and protein-protein interactions. *Cell Commun Signal,* 23(1), p. 142.

Magill, S. S. et al., 2014. Multistate point-prevalence survey of health care-associated infections. *N Engl J Med,* 370(13), pp. 1198-208.

Mariano, L. L. & Ingersoll, M. A., 2018. Bladder resident macrophages: Mucosal sentinels. *Cell Immunol,* Volume 330, pp. 136-141.

Mariano, L. L. & Ingersoll, M. A., 2020. The immune response to infection in the bladder. *Nat Rev Urol,* 17(8), pp. 439-458.

Mariano, L. L. et al., 2020. Functionally distinct resident macrophage subsets differentially shape responses to infection in the bladder. *Sci Adv,* 6(48).

Matico, R. E. et al., 2024. Structural basis of the human NAIP/NLRC4 inflammasome assembly and pathogen sensing. *Nat Struct Mol Biol,* Volume 31, p. 82–91.

Matsushima, N. et al., 2007. Comparative sequence analysis of leucine-rich repeats (LRRs) within vertebrate toll-like receptors. *BMC Genomics,* Volume 8, p. 124.

Mediati, D. G. et al., 2024. Genetic requirements for uropathogenic E. coli proliferation in the bladder cell infection cycle. *mSystems,* 9(10).

Medina, M. & Castillo-Pino, E., 2019. An introduction to the epidemiology and burden of urinary tract infections. *Ther Adv Urol.*

Mittal, R., Chhibber, S., Sharma, S. & Harjai, K., 2004. Macrophage inflammatory protein-2, neutrophil recruitment and bacterial persistence in an experimental mouse model of urinary tract infection. *Microbes Infect,* 6(14), pp. 1326-32.

Murthy, A. M. V. et al., 2018. Regulation of hemolysin in uropathogenic Escherichia coli fine-tunes killing of human macrophages. *Virulence,* 9(1), pp. 967-980.

Naskar, M. & Choi, H. W., 2024. A Dynamic Interplay of Innate Immune Responses During Urinary Tract Infection. *Immune Netw,* 24(4).

Newman, R. M., Salunkhe, P., Godzik, A. & Reed, J. C., 2006. Identification and characterization of a novel bacterial virulence factor that shares homology with mammalian Toll/interleukin-1 receptor family proteins. *Infect Immun,* 74(1), pp. 594-601.

Nielsen, M. C., Andersen, M. N. & Møller, H. J., 2020. Monocyte isolation techniques significantly impact the phenotype of both isolated monocytes and derived macrophages in vitro. *Immunology,* 159(1), pp. 63-74.

Ofir, G. et al., 2021. Antiviral activity of bacterial TIR domains via immune signalling molecules. *Nature,* 600(7887), pp. 116-120.

Ou, Q. et al., 2021. TcpC inhibits neutrophil extracellular trap formation by enhancing ubiquitination mediated degradation of peptidylarginine deiminase 4. *Nat Commun,* 12(1), p. 3481.

Pasi, S., Kant, R. & Surolia, A., 2016. Toll/Interleukin-1 Receptor Domain Derived from TcpC (TIR-TcpC) Ameliorates Experimental Autoimmune Arthritis by Down-modulating Th17 Cell Response. *J Biol Chem,* 291(23), pp. 12358-69.

Porat, R., Clark, B. D., Wolff, S. M. & Dinarello, C. A., 1991. Enhancement of growth of virulent strains of Escherichia coli by interleukin-1. *Science,* 254(5030), pp. 430-2.

Porat, R., Clark, B. D., Wolff, S. M. & Dinarello, C. A., 1992. Response: IL-1β and Escherichia coli. *Science,* 258(5088), pp. 1562-63.

Rajewsky, K., 1996. Clonal selection and learning in the antibody system. *Nature,* 381(6585), pp. 751-8.

Rana, R. R. et al., 2011. Yersinia pestis TIR-domain protein forms dimers that interact with the human adaptor protein MyD88. *Microb Pathog,* 51(3), pp. 89-95.

Rowe, T. A. & Juthani-Mehta, M., 2013. Urinary tract infection in older adults. *Aging health,* 9(5).

Sameer, A. S. & Nissar, S., 2021. Toll-Like Receptors (TLRs): Structure, Functions, Signaling, and Role of Their Polymorphisms in Colorectal Cancer Susceptibility. *Biomed Res Int.*

Santiago-Borges, J. M. et al., 2025. Uropathogenic Escherichia coli niche occupancy determines the effects of mucosal vaccine against FimH. *Cell Rep,* 44(8), p. 116077.

Sato, S. et al., 2003. Toll/IL-1 receptor domain-containing adaptor inducing IFN-beta (TRIF) associates with TNF receptor-associated factor 6 and TANK-binding kinase 1, and activates two distinct transcription factors, NF-kappa B and IFN-regulatory factor-3, in the Toll-like receptor signaling. *J Immunol,* 171(8), pp. 4304-10.

Schubert, S. et al., 2010. Prevalence and phylogenetic history of the TcpC virulence determinant in Escherichia coli. *Int J Med Microbiol,* 300(7), pp. 429-34.

Schultz, T. E. et al., 2025. TLR4 endocytosis and endosomal TLR4 signaling are distinct and independent outcomes of TLR4 activation. *EMBO Rep,* 26(10), pp. 2740-2766.

Schwan, W. R., 2008. Flagella allow uropathogenic Escherichia coli ascension into murine kidneys. *Int J Med Microbiol,* 298(5-6), pp. 441-7.

Shah, C., Baral, R., Bartaula, B. & Shrestha, L. B., 2019. Virulence factors of uropathogenic Escherichia coli (UPEC) and correlation with antimicrobial resistance. *BMC Microbiol,* 19(1), p. 204.

Shah, K., Al-Haidari, A., Sun, J. & Kazi, J. U., 2021. T cell receptor (TCR) signaling in health and disease. *Sig Transduct Target Ther,* Volume 6, p. 412.

Shin, O. S. et al., 2009. Downstream Signals for MyD88-Mediated Phagocytosis of Borrelia burgdorferi Can Be Initiated by TRIF and Are Dependent on PI3K. *The Journal of Immunology,* 183(1), p. 491–498.

Snyder, G. A. et al., 2013. Molecular mechanisms for the subversion of MyD88 signaling by TcpC from virulent uropathogenic Escherichia coli. *Proc Natl Acad Sci U S A,* 110(17), pp. 6985-90.

Snyder, G. A. et al., 2014. Crystal structures of the Toll/Interleukin-1 receptor (TIR) domains from the Brucella protein TcpB and host adaptor TIRAP reveal mechanisms of molecular mimicry. *J Biol Chem,* 289(2), pp. 669-79.

Spear, A. M. et al., 2012. A Toll/interleukin (IL)-1 receptor domain protein from Yersinia pestis interacts with mammalian IL-1/Toll-like receptor pathways but does not play a central role in the virulence of Y. pestis in a mouse model of bubonic plague. *Microbiology (Reading),* 158(6), pp. 1593-1606.

Sun, L. et al., 2023. T cells in health and disease. *Sig Transduct Target Ther,* Volume 8, p. 235.

Takeda, K., Kaisho, T. & Akira, S., 2003. Toll-like receptors. *Annu Rev Immunol,* Volume 21, pp. 335-76.

Ullah, M. O. et al., 2016. TRIF-dependent TLR signaling, its functions in host defense and inflammation, and its potential as a therapeutic target. *J Leukoc Biol,* 100(1), pp. 27-45.

Vejborg, R. M., Hancock, V., Schembri, M. A. & Klemm, P., 2011. Comparative genomics of Escherichia coli strains causing urinary tract infections. *Appl Environ Microbiol,* 77(10), pp. 3268-78.

Verma, V. et al., 2020. α-Hemolysin of uropathogenic E. coli regulates NLRP3 inflammasome activation and mitochondrial dysfunction in THP-1 macrophages. *Sci Rep,* 10(12653).

Ve, T. et al., 2017. Structural basis of TIR-domain-assembly formation in MAL- and MyD88-dependent TLR4 signaling. *Nat Struct Mol Biol,* 24(9), pp. 743-751.

Waldhuber, A. et al., 2016. Uropathogenic Escherichia coli strain CFT073 disrupts NLRP3 inflammasome activation. *J Clin Invest,* 126(7), pp. 2425-36.

Watanabe, S., Kumazawa, Y. & Inoue, J., 2013. Liposomal Lipopolysaccharide Initiates TRIF-Dependent Signaling Pathway Independent of CD14. *PLoS One,* 8(4).

Welch, R. A. et al., 2002. Extensive mosaic structure revealed by the complete genome sequence of uropathogenic Escherichia coli. *Proc Natl Acad Sci U S A,* 99(26), pp. 17020-4.

WHO, 2022. *Global antimicrobial resistance and use surveillance system (GLASS) report 2022.,* Geneva: s.n.

Wicherska-Pawłowska, K., Wróbel, T. & Rybka, J., 2021. Toll-Like Receptors (TLRs), NOD-Like Receptors (NLRs), and RIG-I-Like Receptors (RLRs) in Innate Immunity. TLRs, NLRs, and RLRs Ligands as Immunotherapeutic Agents for Hematopoietic Diseases. *Int J Mol Sci,* 22(24), p. 13397.

Yadav, M. et al., 2010. Inhibition of TIR domain signaling by TcpC: MyD88-dependent and independent effects on Escherichia coli virulence. *PLoS Pathog,* 6(9).

Yang, X. et al., 2022. Disease burden and long-term trends of urinary tract infections: A worldwide report. *Front Public Health.*

Zhong, Y., Kinio, A. & Saleh, M., 2013. Functions of NOD-Like Receptors in Human Diseases. *Front Immunol,* 4(333).

Zhou, J., Zhuang, Z., Li, J. & 1, Z. F., 2023. Significance of the cGAS-STING Pathway in Health and Disease. *Int J Mol Sci,* 24(17), p. 13316.